

**THE STUDY OF POLYPROPYLENE - HYDROUS
MAGNESIUM SILICATE COMPOSITE AS AN ELECTRET**

BY

SYED JAMAL AHMED

SUBMITTED IN PARTIAL FULFILMENT
OF THE REQUIREMENTS FOR THE
DEGREE OF M. PHIL.



DEPARTMENT OF PHYSICS
BANGLADESH UNIVERSITY OF ENGINEERING AND TECHNOLOGY

DHAKA- 1000

August, 1996



**BANGLADESH UNIVERSITY OF ENGINEERING AND TECHNOLOGY,
DHAKA**

DEPARTMENT OF PHYSICS

Certification of Thesis work

A Thesis on

**THE STUDY OF POLYPROPYLENE-HYDROUS MAGNESIUM SILICATE
COMPOSITE AS AN ELECTRET**

BY

Syed Jamal Ahmed


has been accepted as satisfactory in partial fulfilment for the degree of Master of Philosophy in Physics and certifying that the student demonstrated a satisfactory knowledge of the field covered by this thesis in an oral examination held on January, 26, 1997.

Board of Examiners

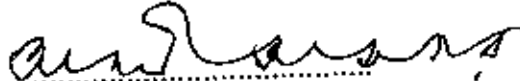
1. Dr. Md. Abu Hashan Bhuiyan
Associate Professor of Physics
BUET, Dhaka.


Supervisor & Chairman

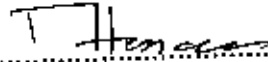
2. Head
Department of Physics
BUET, Dhaka.


Member

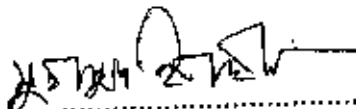
3. Prof. M. A. Asgar
Department of Physics
BUET, Dhaka.


Member

4. Prof. Tafazzal Hossain
Department of Physics
BUET, Dhaka.


Member

5. Dr. M. Ibrahim
Professor, Department of Physics
University of Dhaka
Dhaka.


Member (External)

CERTIFICATE

This is to certify that the author is solely responsible for the work reported in this thesis and this work has not been submitted to any university or elsewhere for the award of a degree or diploma.

Syed Jamal Ahmed

Candidate

(SYED JAMAL AHMED)

Roll No. 9111F

Session : 1989-90

Abu Hashan Bhuiyan

Supervisor

(DR. MD. ABU HASHAN BHUIYAN)

Associate Professor

Department of Physics

BUET, Dhaka.

ACKNOWLEDGMENT

I would like to express my deepest gratitude to my reverend teacher Dr. Md. Abu Hashan Bhuiyan, Associate Professor, Department of Physics, Bangladesh University of Engineering & Technology, Dhaka for his continuous supervision, valuable suggestions and encouragement during my research work.

My deep sense of gratitude is due also to Dr. Gias Uddin Ahmad, Professor and Head, Department of Physics, Bangladesh University of Engineering & Technology, Dhaka for his kind co-operation and inspiration during the work.

I also express my gratitude to Professor Dr. Tafazzal Hossain, Professor Dr. M. Ali Asgar and Professor Dr. Mominul Huq of the same department for their encouragement during the work.

I am grateful to Dr. J. Podder and Dr. Feroze Alam, Assistant Professors of the department for their inspiration during the work.

I express my indebtedness towards my uncle Syed Salim and aunt Chuni Chowdhury for their inspiration to complete the thesis work.

My thanks are due to the members of DigiCon Computers for their help in computer composing of the thesis.

I am grateful to my friends Tapan and Mukta for their help.

Finally, I am grateful to my parents for their encouragement that made the whole project possible.

ABSTRACT

Polypropylene - Hydrous Magnesium Silicate (Talc) (PP-Talc) composites with different PP and Talc composition (wt%) were prepared by extrusion method. The UV-visible absorption spectroscopic and thermally stimulated depolarization current (TSDC) measurements were carried out on the pure PP and five different PP-Talc composites.

From the UV-visible absorption studies, the bandgap of PP and PP-Talc composites were calculated from absorption versus photon energy graph. The absorption shows presence of defects/ impurities in the materials.

The TSDC technique was used to study the charge storage and charge relaxation behaviour in pure PP and PP-Talc composites. The TSDC thermograms show two distinct and wide peaks in the temperature regions 285-323 and 400-410K. The incorporation of Talc in PP shifts both the peaks towards low temperature. The low temperature peak in the composites is due to the existence of Talc in PP together with the result of some mode of polymer motion.

An analysis of the dependence of total released charge, Q , on polarizing voltage, V_p , and Talc content (wt%) show that the relaxation is dipolar but the polarization is restricted by the repulsion force between the cations with the increase of Talc content (wt%) in PP. The variation of peak current with polarizing voltage, V_p , and Talc content (wt%) are also presented. The increase of activation energy with Talc content (wt%) also supports the above facts.

CONTENTS

CHAPTER-I	INTRODUCTION	PAGE
1.1	Materials with improved physical properties	1
1.2	Composites	2
1.2.1	Properties and applications	3
1.3	Polymer	4
1.3.1	Types of polymer	4
1.3.2	Glass transition temperature of polymer	7
1.4	Polypropylene	11
1.4.1	Properties and applications	11
1.5	Hydrous Magnesium Silicate (Talc)	12
1.5.1	Properties and application	12
1.6	Objectives of the present work	14
	References	15
CHAPTER-II	THEORETICAL BACKGROUND	
2.1	Introduction to thermally stimulated depolarization current (TSDC) method	16
2.2	Polarization mechanisms	17
2.3	Theory of thermally stimulated depolarization current	18
2.3.1	Dipolar TSDC in dielectric with a single relaxation time	19
2.3.2	Determination of activation energy	21
2.3.3	TSDC involving space charge processes	21
2.3.4	TSDC involving interfacial processes	23
2.3.5	The equivalent frequency of TSDC measurements	24
2.4	UV-Visible optical absorption spectroscopy	24
2.5	Literature review	26
	References	31

CHAPTER-III	EXPERIMENTAL DETAILS	PAGE
3.1	Raw materials used in this research work	33
3.2	Details of the fabricated extrusion machine set up in the laboratory	34
3.3	Preparation of the different samples	38
3.4	Electrode deposition	38
3.5	UV-Visible optical absorption spectroscopy	40
3.6	Instruments used in TSDC measurements	40
3.7	TSDC measurements	44
3.7.1	General procedure for TSDC measurements	44
3.7.2	The present TSDC measurements	44

CHAPTER-IV	RESULTS AND DISCUSSION	
4.1	UV-Visible optical absorption spectra	52
4.2	Thermally stimulated depolarization current (TSDC) measurements	63
4.2.1	TSDC spectra for pure PP	63
4.2.2	TSDC spectra for composites	66
4.2.3	Dependence of the total charge Q released on the Vp and Tale content (wt%)	78
4.2.4	Activation energy from TSDC	80
	References	86

CHAPTER-V	CONCLUSIONS	
5.1	Conclusions	87
5.2	Suggestions for further study	88

Appendix

CHAPTER-I

INTRODUCTION

- 1.1 Materials with improved physical properties
- 1.2 Composites
 - 1.2.1 Properties and applications
- 1.3 Polymer
 - 1.3.1 Types of polymer
 - 1.3.2 Glass transition temperature of polymer
- 1.4 Polypropylene
 - 1.4.1 Properties and applications
- 1.5 Hydrous Magnesium Silicate (Talc)
 - 1.5.1 Properties and application
- 1.6 Objectives of the present work
- References



Chapter-I

Introduction

1.1 Materials with improved physical properties

It is possible now-a-days to make various engineering new materials from traditional material; for example a ferromagnet from a plastic, a super conductor from a ceramic, a spring from Portland cement. The new materials which have achieved prominence on the technological arena in the last few decades are Composites, Polymers, Ceramics etc. Compositing is shown to be a unifying influence in designing new materials for specific functions. Composites have acquired a leading position in the development of new materials because of the realization that with judicious choice of combinations of materials startling new combinations of properties can be obtained. Composites are best known for their mechanical properties. The stiffest and strongest materials known or believed to be possible consist of the elements and binary compounds of the covalently bound solids. Fibrous composite materials, particularly glass reinforced plastic have been used for many years. The new advanced composites are being designed for much more sophisticated and demanding application. The principle of compositing materials is used in a very sophisticated way in bandgap engineering in microelectronics.

New materials can be produced by the synthesis of diamond and very hard carbon at normal pressures on a substrate at room temperature without a seed from radio frequency and microwave frequency plasmas using hydrocarbons plus hydrogen as a source gas. The mechanical, electrical and optical properties of such films are as exciting as the production of superconductors operating above 77K [1.1]

Polymers are all based on carbon and are designed at a molecular level to control the average length of the chains, the strength of the forces between the chains, the stiffness of the individual chains and the regularity with which the chains are packed together. Recent advances are in processing the chains to achieve starting increases in the stiffness by

achieving full alignment. The other new approach to polymeric materials is to form blends, composites which are immiscible and by heating and cooling to form particles of one polymer in the matrix of another.

Finally with metallic glasses available, plastic as strong and stiff as metals, with metals being formed like plastics and plastics shaped like metals, with ceramics showing high heat conduction and plastics conducting electricity often emphasized in physics. This is having striking engineering consequences.

1.2 Composites

Most naturally occurring materials derive their superb properties from a combination of two or more components which can be distinguished rapidly when examined in optical and electron microscope. The composite idea is particularly relevant to engineering components which may consist of two or more materials combined to give performance in service which is superior to the properties of the individual materials.

The definition of a composite material is difficult and there is no really adequate definition of a composite material. Basically a composite can be defined as the material created when at least two different, relatively homogeneous phase, i.e. the material and the dispersed phase, are combined to produce a homogeneous material of a more complex structure, having properties which are not obtainable by any of the constituents acting alone. The constituent materials are separated by a less clearly defined phase known as the interface.

Three main points can be included in a definition of an acceptable composite material.

- I) It consist of two or more physically distinct and mechanically separable materials.
- II) It can be made by mixing the separate materials in such a way that the dispersion of one materials in the other can be done in a controlled way to achieve optimum properties.

- III) The properties are superior and possibly unique in some specific respects, to the properties of the individual components.

Generally composite materials can be divided into three classes:

- a) Dispersion -reinforced composite materials e.g. Aluminum dispersed in silver.
- b) Particulate- reinforced composite materials e.g. Rubber reinforced with carbon black.
- c) Fiber- Reinforced composite materials e.g. Epoxy design or polyester reinforced with glass fibers.

Natural Composite materials are wood bone, bamboo etc.

Microcomposite materials are steel, polystyrene etc.

Macrocomposite materials are galvanized steel, reinforced concrete beams helicopter blades etc

1.2.1 Properties and Applications

Composite materials have strongest interatomic bonds coupled with deep interatomic potential wells, implying large sublimation energies. Composite materials are the strongest stiffest materials of least density. The stiffness is easily appreciated but the higher tensile strength can only be observed if the material is in the form of a fiber. Composite material provides Young moduli of up to 700 to 800 Gpa. Metal matrix composites have lower thermal expansion co-efficient, higher thermal conductivity, dimensional stability, no deterioration under hot and wet conditions, little material loss in high vacua, no low temperature brittleness and resistance to radiation damage. Ceramic - Ceramic composites have good chemical compatibility at high temperature.

Composite materials have many application in the various industrial, domestical and electrical uses. Fibrous composites have demanding application in aerospace, in medicine and in sports goods. The wings of AV8B (Harrier) aircraft are made of graphite fiber in a woven form in an epoxy resin. Metal matrix composites finds application in wear

resistant. Composite materials are used as electrical insulators and stable encapsulates for electrical circuits.

1.3 Polymer

Polymers are the substances which are made up of large molecules or macromolecules. These macromolecules or giant molecules are composed of repetition of small repeating units which are called "monomer". Polymers may be natural or artificially synthesized. Natural polymers exist in plants and animals and include starch, proteins, lignin, cellulose, collagen, silk and natural rubber etc. Synthetic polymers derived mainly from oil based products include polyethylene (PE), nylon, epoxies, phenolic and synthetic rubber etc.

1.3.1 Types of Polymer

a) Homochain polymer

When polymers are made in chain reactions containing only carbon atoms in the main chain called homochain polymers.

b) Heterochain polymer

The types of polymers made in step reaction may have other atoms, originating in the monomer functional groups, as part of the chain, called the heterochain polymers.

c) Steric isomer

When the repeat unit of a polymer chain are themselves asymmetric, on account of their containing a carbon atom with four different substituents, the large numbers of possible permutations of right handed and left handed units represents a large numbers of steric

isomers. This kind of isomerism in polymer is called tacticity. There are three main types of steric isomers

i. Isotactic

In this isomer all repeat units are identical, either right handed or left handed form and arranged in linear, head to tail fashion. In the fully extended chain all the methyl substituents lie on the same side of the chain.

ii. Syndiotactic

Here successive repeat units alternate in configuration $dlldll\dots$, and successive methyl groups along the fully extended chain lie on alternate sides. More elaborate ordering does not often occur in practice.

iii. Atactic

This describes a completely random arrangements of the repeat units d and l along the chain.

d) Thermosetting polymer

Thermosetting polymer systems are based and characterized by an initial state of low viscosity, which on curing leads to an chemically irreversible hardened cross-linked brittle material exhibiting low strain to failure but high stiffness and yield strength. In the thermosetting field cross-linked polyester resins phenol - formaldehyde resins (phenolics), melamine - formaldehyde resins (melamines), epoxides and silicon resins are among the most commonly used. The thermosetting plastics have superior abrasion and dimensional stability characteristics compared with the thermoplastics. Thermosetting

polymers are changed irreversibly from fusible, soluble products into highly interactable cross-linked resins which cannot be molded by flow and so must be fabricated during the cross linked process. Thermosetting resins are usually isotropic. Their most characteristic property is in response to heat since, unlike thermoplastics, they do not melt on heating. However they lose their stiffness properties at the heat distortion temperature and this defines an effective upper limit for their use in structural components. Epoxy resins are generally superior to polyester resins in this respect but other resins are available which are stable at higher temperatures such as aromatic polyamides and polyimides.

e) **Thermoplastic polymer**

To discuss all the thermoplastics that potentially could or have been utilized as matrices in composite materials would mean mentioning nearly every commercially available products which are reinforced include nylon, polyethylene (PE), polypropylene (PP), polycarbonate (PC), polystyrene, styreneacrylonitrile and the acetals. Unlike thermosetting resins, thermoplastics are not cross linked. They derive their strength and stiffness from the inherent properties of the monomer units and the very high molecular weight. This ensures that in amorphous thermoplastics there is a high concentration of molecular entanglements, which act like cross-linked, and in crystalline materials there is a high degree of molecular order and alignment. In amorphous materials heating leads to disentanglement and a change from a rigid solid to a viscous liquid. In crystalline materials heating results in melting of the crystalline phase to give an amorphous viscous liquid. Both amorphous and crystalline polymer may have anisotropic properties depending on the conditions during solidification. In amorphous polymers this is due to molecular alignment which occurs during melt flow in molding the material or subsequently during plastic deformation. Similarly, in crystalline polymers the crystalline lamellar units can develop a preferred orientation due, for example, to non-uniform nucleation at surfaces or in the flowing melt and preferential growth in some directions because of temperature gradients in the melt. The characteristic ability to melt and

reform has led to this class of polymer being used in high productivity molding applications.

Like many other materials the polymeric materials can be divided into two groups on the basis of the presence of permanent dipole moments. These are (i) Polar polymer and (ii) non polar polymer.

(a) Polar polymer

Polymers which possess permanent dipole in the absence of any external electric field then it is said to be polar polymers. The examples of polar polymers are polyamides, polyvinylchloride, polytetrafluoroethylene. In a polar polymer strong polymer-polymer bonds usually develop that causes the solubility of the polymer to decrease. For polar polymers the dielectric constant and dielectric loss are comparatively higher than non polar polymers.

(b) Non polar Polymer

These are the polymers which have no permanent dipole moment in the absence of external electric field. These are flexible and have pendent side groups which can rotate freely. The density of non polar polymer covers a range depending on the extent of chain branching which determines its crystallinity. Pure non polar polymers show no dipole relaxation effects, therefore having low dissipation factor. These polymers have low dielectric constant also.

1.3.2 Glass transition temperature of Polymer

The glass transition temperature is the temperature at which the molten polymer changes to a hard glass. This transformation occurs over a temperature range that includes the glass temperature, T_g . There is a small temperature region about T_g in which the polymer viscosity varies rapidly with temperature from a very high viscosity

characteristics of a glass to a low viscosity characteristic of a more or less viscous liquid. It is the temperature region in which the thermal motion of the molecules become so slow that they are unable to respond within a responsible time to the action of an applied force. Consequently, the material is observed to change from a soft to a hard substance as the temperature is lowered through this region. The glass transition generally occurs in the amorphous state. It does not correspond to any change in the atomic structure. Below T_g , the characteristic relaxation time, τ of the molecule is large, while above T_g , it is small.

In the temperature interval between T_g and the melting point of the crystal T_m , the material could be said to be in a super cooled liquid state and is so viscous that it appears solid, whereas below T_g , the material is solid. Such situation is shown in the figure 1.1. in the cases of the coefficient of expansion and the specific heat capacity : below T_g , the values of one close to those of the crystal, above T_g , to those of the liquid.

When the transitions additional to T_g (and to T_m with crystalline polymer) became apparent it became conventional to label the highest transition (other than T_m where this exists) as an α transition, labeling other transitions β, γ, δ etc., in decreasing order of temperature. In most cases, but not always, the glass transition temperature corresponded to the α transition. such a formal nomenclature ignored the physical reagents for a transition and it is not surprising that the reason for different transitions vary from one polymer to another. Some mechanism may be common to several materials, others may be highly specific. Hence, a so called β - transition in one polymer may have a quite different origin than a β - transition in a second polymer. At the same time the β - transition the first polymer could have e.g., the same physical origin as a so called γ - transition in the second polymer. The nomenclature α, β, γ is therefore only a method of labeling a given polymer and no special significance should be attached to such a term as β - transition or γ - transition without reference to a given polymer.

In amorphous polymers transitions occur where, because of an increase in temperature, a point is reached where the molecules gain sufficient energy to indulge in additional

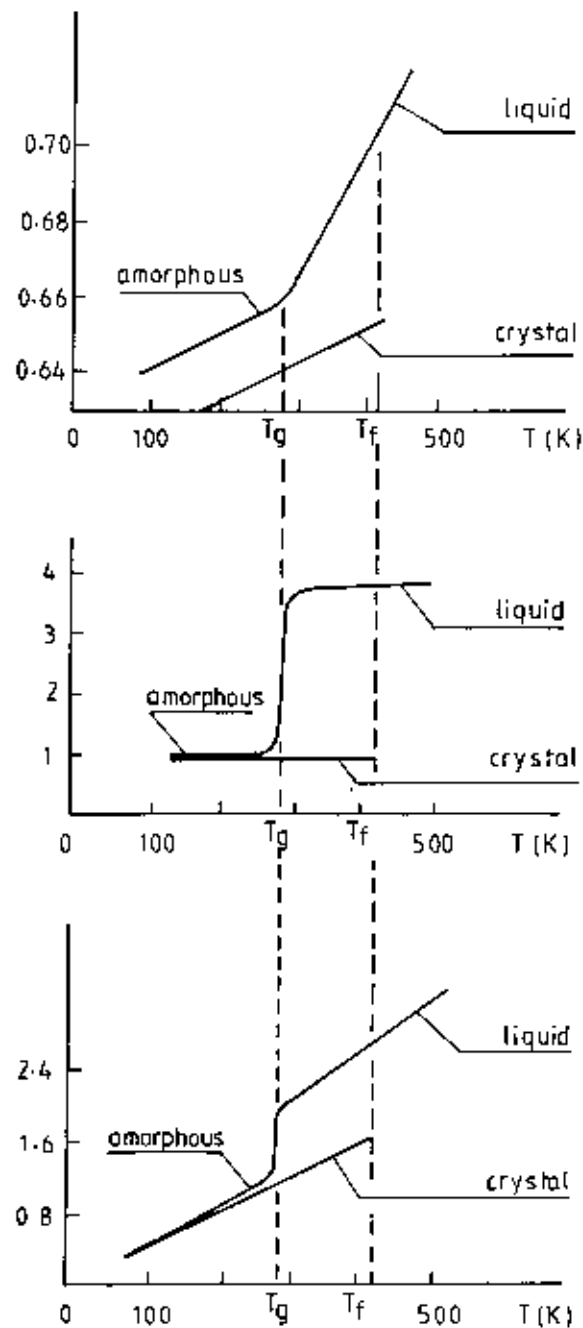


Fig. 1.1: Defining the glass transition temperature T_g in (a) the volume per unit mass (b) the co-efficient of expansion and the specific heat capacity for glucose which exists in both the amorphous and crystalline states.

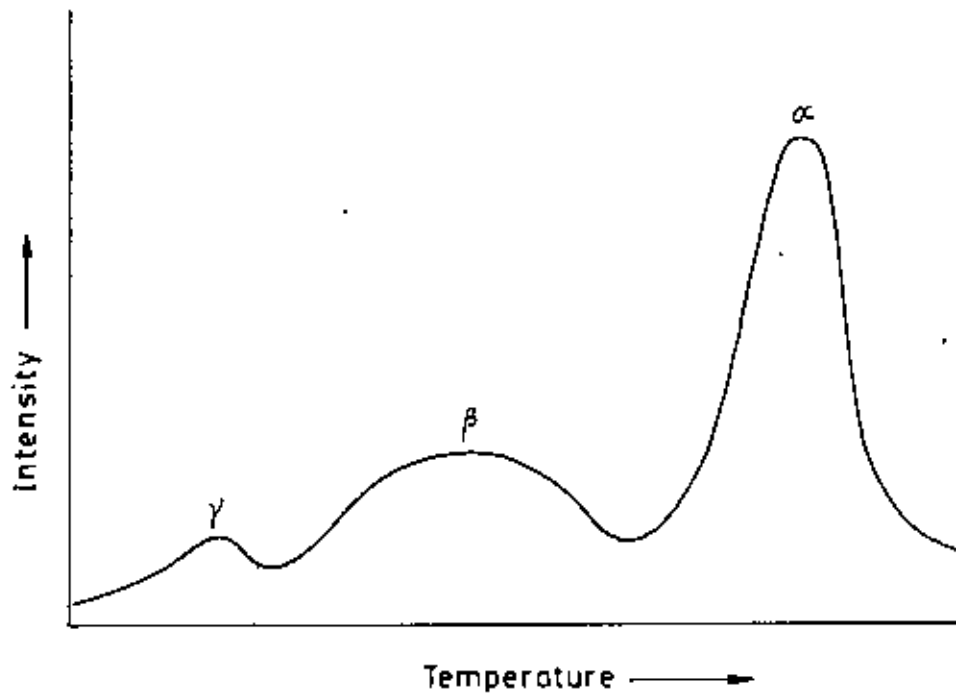


Fig. 1.2: Different transition regions in a TSDC spectrum

motions . With such amorphous material five types of transition appear possible. In order of increasing temperature they are:

- i) Motion of a side group , e.g., methyl, about an axis at axis at right angles to the chain .
- ii) Motion of two to four carbon moieties in the main chain (the Schatzki crankshaft effect).
- iii) Motion of moieties containing hetero-atoms in the main chain, e.g., the amide group in a polyamide .
- iv) Motion of a chain segments of about 55-100 backbone atoms (which corresponds to T_g).
- v) Motion of the entire chain as a unit.

1.4 Polypropylene

Polypropylene(PP), a thermoplastic, is chemically similar to Polyethylene(PE) but have somewhat better physical strength at a lower density. The density of polypropylene is among the lowest of all plastic materials. PP have an almost infinite life under flexing perhaps the only thermoplastic surpassing all others in combined electrical properties, heat resistance, rigidity toughness, chemical resistance, dimensional stability, surface gloss and melt flow, at a cost less than that of most others.

1.4.1 Properties and Applications

Polypropylene is soluble in only boiling aromatic hydrocarbons such as toluene and xylene. It has high temperature resistance. It has high compressive strength, tensile strength, mechanical strength and impact strength. It has good dimensional stability under stress and high abrasion resistance. The thermodynamic melting point of pure crystalline PP is 460K. PP has low specific gravity and it is resistant to chemicals. It is attacked by oxidizing agent. PP being nonpolar, it has good dielectric property even at high frequency.

Because of their exceptional quality and versatility, polypropylene offer outstanding potential in the manufacture of products through injection molding. Polypropylene are used for packing; squeeze type bottles, production of pipes, tanks, textile machinery parts and insulating electric wires etc.

1.5 Hydrous Magnesium Silicate (Talc)

Natural minerals are termed as Talc. It is hydrous magnesium silicate having the chemical formula $Mg_3SiO_{10}(OH)_2$. Talc contains 31.7% MgO, 63.5% SiO_2 and 4.8% H_2O . Talc deposits are probably formed by hydrothermal alteration or contact metamorphism of preexisting rocks. Talc is found in many parts of the world. The united states is the largest producer. [1-2,1.3].

1.5.1 Properties and Applications

The characterization of a pure Talc mineral is done by its softness, hydrophobic surface properties and slippery feel [1.4.1.5,1.6]. The crystal form may be foliated, lamellar, fibrous or massive. Commercially available Talcs are harder, due to the presence of impurities. Crude Talcs range in colour from white to green and brown. In powder form pure Talcs are of white colour. The refractive index of Talc is 1.54-1.59 and specific gravity is 2.7-2.8. Pure Talc is heat stable up to 1173K. Talc is inert in most chemical reagents although it exhibits a marked alkalinity ($P^H = 9-9.5$). It is soluble in hot concentrated Phosphoric acid (H_3PO_4). It has very low cation exchange capacity. Talc prevents delayed glaze crazing, lowers firing temperature and reduces fired shrinkage [1.7]

Talc is the basic raw materials used to enhance opacity and printing properties. The paper industry is the largest consumer of Talc. It is used in the pulp and paper making process. Talc is used in ceramics, electrical ceramics. As the Talc is low loss insulator, it is used in a wide variety of electronics and electrical uses. The next most important

application is in protective coatings. Talc also used as insecticide carriers, rubber dusting and textile filling materials and as additive in asphalt roofing compounds. More recently, the use of talc for plastics filling and reinforcement has grown rapidly [18]. Polypropylene parts reinforced with as much as 40% Talc have replaced metal in many automotive applications. Polypropylene replacement for metal in domestic applications represents another important new market for Talc. Catalytic converters for automotive pollution control have also become important talc consumers since mid 1970's.

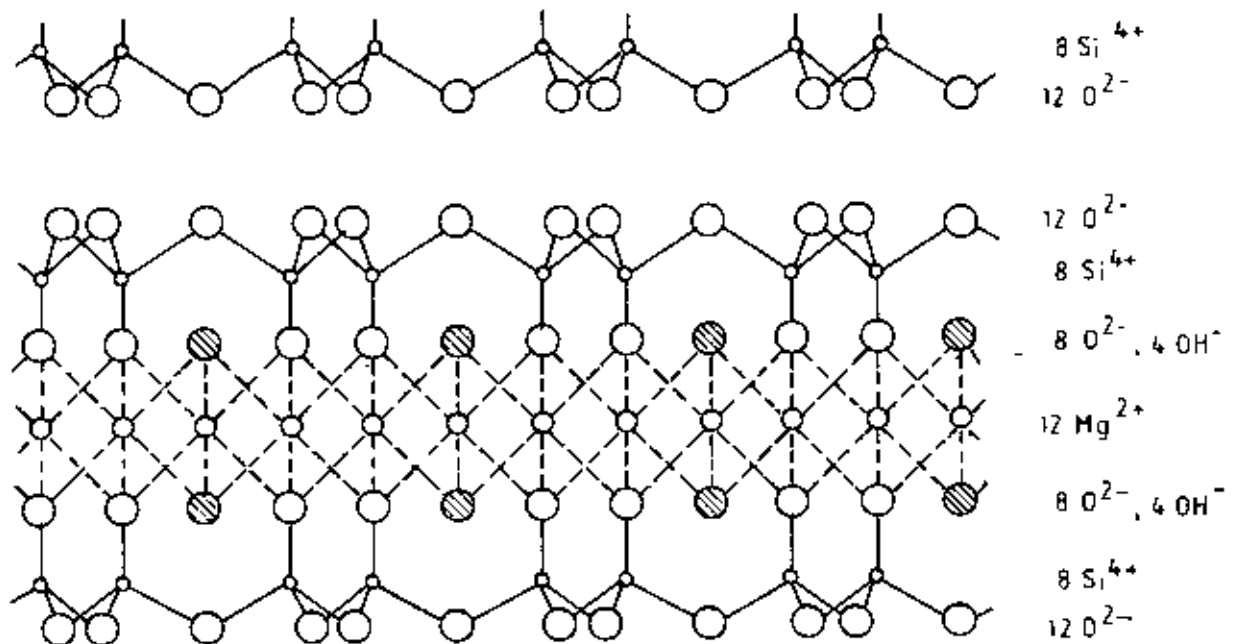


Fig. 1-3: Crystal structure of pure Hydrous Magnesium Silicate (Talc).

1.6 Objectives of the present work

The conventional physical properties of the traditional materials, such as, metal, polymers etc. are not adequate to fulfill new technological requirements . These limitations dictate search for new materials with improved properties. One way to achieve this goal is to obtain composite materials having superior properties compared with that of the traditional ones. Polymer matrix composites offer great versatility of application and considerable simplicity and convenience in the manufacture of artefacts.

Charge storage and charge transport, which determine the electrical properties of polymer are affected by additives or fillers in polymers. Polypropylene (PP), a thermoplastic, is known for its good thermal stability . One of the important reasons for the increasing use of PP in technical applications is the possibility to vary its properties by a wide scale of Compounding and Blending techniques[1.9]. Composites of PP are promising new materials with improved properties and may find scientific applications.

In order to find use in the electrical application, it is necessary to study the charge storage and transport behaviour of PP-Talc composite electrets. Keeping this view in mind, in the present investigation PP-Talc of different composition are considered. Thus the following objectives are brought under the present scheme of study.

- i. Preparation of PP-Talc composites of different composition .
- ii. Optical studies of the composites by UV-VIS absorption spectroscopy.
- iii. Study of the storage and transport behaviour by thermally stimulated decolorization current (TSDC) technique.
- iv. Finally, the physical processes involved in the electret for charge storage and transport will be discussed

References of chapter - I

- 1.1 New materials and their applications. 1987 edited by S.G Burnay, Institute of physics conference series number 89.
- 1.2 Minerals Year book, U.S Dept. of interior, Bureau of Mines. U.S. Government printing office, Washington D.C., 1980.
- 1.3 R.A. Cerflon, Mineral facts and problems, Bulletin 671, U.S. Bureau of Mines, Washington D.C. (1980), 1-12.
- 1.4 M Ross. J. Am. Min. 53, (1968) 751.
- 1.5 G.W. Brintley and I S. Stemple. J. Am. Cer. Soc., 37 (3) (1960) 118.
- 1.6 J A. Pask and M.F. Warner , J Am cer. soc. 37 (3)(1954)118.
- 1.7 W.W. Gaskins , J.Am. Cer. Soc. Bulletin, 31 (10) (1952) 392.
- 1.8 J.A. Radota and N.C. Trivedi, Handbook of fillers and Reinforcement plastics (1978)160 -171.
- 1.9 A. M. Rifeley, C.D. Paynter, P M. McGenity and J. M. Adams, Plastics Rubber Proc. Appl., 14 (1990) 85.

CHAPTER-II

THEORETICAL BACKGROUND

- 2.1 Introduction to thermally stimulated depolarization current (TSDC) method
 - 2.2 Polarization mechanisms
 - 2.3 Theory of thermally stimulated depolarization current
 - 2.3.1 Dipolar TSDC in dielectric with a single relaxation time
 - 2.3.2 Determination of activation energy
 - 2.3.3 TSDC involving space charge processes
 - 2.3.4 TSDC involving interfacial processes
 - 2.3.5 The equivalent frequency of TSDC measurements
 - 2.4 UV-Visible optical absorption spectroscopy
 - 2.5 Literature review
- References

Chapter -II

Theoretical Background

2.1 Introduction to Thermally Stimulated Depolarization Current (TSDC) Method

The method of thermally stimulated depolarization currents (TSDC) is a general method of investigating the electrical properties of high - resistivity solids via the study of thermal relaxation effects.

TSDC is developed by heating a polarized sample up to or above the polarization temperature, the release of charge is gradually sped up and, when the half-life of this process becomes comparable with the time scale of the experiment (determined by the heating rate) discharge becomes measurable and gives rise in the external circuit to a current which first increases with increasing temperature and then decays when the supply of charges is depleted. A current peak thus will be observed at a temperature where dipolar disorientation, ionic migration or carrier release from traps is activated etc. and, as the total polarization usually arises from a combination of several individual effects with various relaxation times.

Basically TSDC consists of measuring depolarization currents with a definite heating scheme. The current generated by the build up and / or the release of a polarized state in a solid dielectric sandwiched between two electrodes. The general experimental procedure usually involves four step. [2.1]

- a) the application of a d.c bias V_p at a polarizing temperature T_p for a time t_p
- b) cooling under this bias to some lower temperature T_0
- c) removal of the bias at T_0 to another value V_d
- d) heating at a constant rate while maintaining the sample at zero bias and recording the discharge current as a function of temperature.

Thus the current peaks are observed during the thermally stimulated activated transition from the polarized state to the equilibrium state: this technique is generally known as the ionic thermocurrent (ITC) technique or thermally stimulated depolarization current technique (TSDC). This technique for studying charge motion in solid dielectrics are based on thermally activated release or trapped electron charge or polarization from the localized energy levels [2.2.2.3]. The source of the thermally stimulated current may be.

- i. The thermal release of trapped electrons, holes, ions.
- ii. some type of orientational (dipole) polarization
- iii. space charge polarization.
- iv. interfacial polarization

If a material contains several traps of different energy, then a corresponding number of current peaks should be observed during heating.

2.2. Polarization mechanisms

The polarization of the solid dielectric submitted to an external electric field may occur by a number of mechanism involving, microscopic or macroscopic charge displacement.

- I. The electronic polarization which results from the deformation of the electronic shell and it is the fastest process requiring about 10^{-15} s.
- II. The atomic polarization which results from the atomic displacement in molecules with heteropolar bonds requiring about 10^{-14} to 10^{-12} s.
- III. The orientational or dipolar polarization occurs in materials containing permanent molecular or ionic dipoles requiring as low as 10^{-12} s or long that no relaxation is observed.
- IV. The translational or space charge polarization which is observed in materials containing intrinsic free charges (ions or electrons or both) is due to a macroscopic

charge transferred towards the electrodes action as total or partial barriers. The time required can vary from milliseconds to years.

- V. The interfacial polarization or Maxwell-Wagner-Sillers (MWS) polarization which is characteristics of system with a heterogeneous structure. It results from the formation of charge layers at the interfaces, due to unequal condition currents within the various phases. The time scale is also from milliseconds to years.

2.3 Theory of Thermally Stimulated Depolarization Current

Until recently many authors worked on TSDC technique. They have essentially applied TSDC measurements to the study of electrets i.e. permanently charged dielectric. They made use of an arbitrarily programmed temperature rise. It was Bucci and Fieschi first gave a theoretical basis of the TSDC phenomenon to study the dipolar polarization due to noninteracting point defect dipoles in ionic crystal [2.2]. This method contributed substantially to a better understanding of the role that dipolar imperfections play in affecting a variety of processing in ionic crystals. Historically, the study, the study of thermally activated process by means of the thermal release of stored energy was introduced first in thermoluminescence (TL), then employed in the thermal release of trapped electronic charge to determine the distribution of trapping in photoconductors, in the presence of external field. The TSDC procedure there after received a number of confusing terms due to the fact that it was reinstituted and developed by several investigations using quite different starting points and who most of the time, were not aware of preceding work in the field such as electret thermal analysis, thermally stimulated depolarization, thermally stimulated discharge, thermal current spectra, thermally activated depolarization.

Here the purpose is to outline the more general theories related to the main polarization processes (dipolar, space charge and interfacial polarizations). The emphasis is given to the most commonly used TSDC technique.

2.3.1 Dipolar TSDC in dielectric with a single relaxation time

The structural interpretation of dielectric relaxation processes occurring in many polar materials is usually approached by assuming impaired motions or limited jumps of permanent electric dipoles. The first theory of TSDC applied to dipolar processes was put forward in 1964 by Bucci and Fieschi [2.2]. In this theoretical treatment the polarized material is assumed to be free of charge carriers, so that internal field and the dipolar polarization can be considered as space independent. Practically, dipolar and space-charge polarizations often coexist, particularly in thermoelectrets formed at higher temperature and the electric field and polarization must than be considered as averaged over the thickness of the sample[2.3]. Furthermore the simultaneous displacement of free charge carriers on dipoles during the polarization process may lead to a particular situation where the internal electric field is nearly zero, so that no preferred orientation of dipoles occurs. On the otherhand this implies that after removing the voltage at low temperature, an internal electric field, due to the fixed space charges, exists inside the sample and there, during the subsequent heating, this field will be responsible for a gradual orientation of the dipoles, leading to a current peak quite similar to a true disorientational peak[2.4].

The build up of polarization P in a unit volume of the material during time t after the application of an electric field E_p at a temperature T_p is an exponential function of time,

$$P(t) = P_e \left[1 - \exp\left(-\frac{t}{\tau}\right) \right] \quad (2.1)$$

Where τ is dipolar relaxation time and $P_e = sN_d p_\mu^2 \kappa F_p / kT_p$ is the equilibrium polarization. In this expression s is a geometrical factor, N_d the concentration of dipoles, p_μ their electrical moment, k Boltzmann's constant and κF_p the local directing electric field.

The decay of polarization after removal of the field at $t = \infty$ is

$$P(t) = P_e \exp\left(-\frac{t}{\tau}\right) \quad (2.2)$$

and the corresponding current density

$$J(t) = \frac{dP(t)}{dt} = \frac{P(t)}{\tau} \quad (2.3)$$

The temperature variation of relaxation time is given by

$$\tau(t) = \tau_0 \exp\left(\frac{E}{kT}\right) \quad (2.4)$$

Where τ_0 is the relaxation time at infinite temperature, E is the activation energy of dipolar orientation.

The current density $J_D(T)$ during TSDC experiment is

$$J_D(T) = \frac{P_e(T_p)}{\tau_0} \exp\left(-\frac{E}{kT}\right) \exp\left[-\frac{1}{q\tau_0} \int_{T_0}^T \exp\left(-\frac{E}{kT}\right) dT\right] \quad (2.5)$$

Here, q the heating rate. The first exponential dominates in the low temperature range, is responsible for the initial increase of the current with temperature while the second exponential dominates at high temperature gradually slows down the current rise.

Differentiating eqn. (2-5) it can be arrived at the maximum temperature of the peak (T_m)

$$T_m = \left[\frac{E}{k} q \tau_0 \exp\left(\frac{E}{kT_m}\right) \right]^{\frac{1}{2}} \quad (2.6)$$

Here q is the heating rate, eqn (2-6) shows that dipolar TSDC peak will be an increasing function of the parameters Q , τ_0 and E .

2.3.2 Determination of activation energy

The activation energy of a nondistributed relaxation process can be easily calculated from a single TSDC experiment by means of some characteristic elements of the peak such as its half width, inflection point or initial rise method of Garlick and Gibson[2.5] is based on the fact that the internal term in $J_D(T)$ function being negligible at $t \ll \tau_m$. The first exponential dominates temperature rise of the initial current, so that

$$\ln J_D(T) = \text{Const.} - \frac{E}{kT} \quad (\text{Arrhenius shift}) \quad (2.7)$$

$$= \text{Const.} + \ln T - \frac{E}{kT} \quad (\text{Eyring shift}) \quad (2.8)$$

$$= \text{Const.} - \frac{E_w}{k(T-T_\infty)} \quad (\text{WLF shift}) \quad (2.9)$$

The activation energy can be determined with good accuracy by plotting $\ln J_D(t)$ against $1/T$ or $1/(T-T_\infty)$. A straight line is obtained whose slope gives $-E/k$.

2.3.3 TSDC involving Space Charge Processes

The theory of space-charge polarization is very intricate. Two basic models are usually considered as starting points for a TSDC theory : In the charge motion model the current is assumed to be governed by the bulk conductivity of the material (electronic or ionic), irrespective of its possible trapping properties, while in the trapping model, the current is assumed to result only from carriers (usually electronic) released into the conduction (or valence) band as the charge distribution returns to equilibrium.

The space charge polarization i.e. the polarization due to excess charges which cause the material to be spatially not neutral is a much more complex phenomenon than the dipolar polarization.

In heterocharged dielectric where the presence of space charges arises from field induced transport of pre-existing and /or field generated charge carriers. For depolarization process carrier drift occurs under the influence of local electric fields.

The current density eqn. obtained by Muller [2.4] is given as

$$J_D(T) = \frac{K\sigma_0 P(T_0)}{\epsilon_0 \epsilon_1} \exp\left[-\frac{E}{kT} - \frac{K\sigma_0 k}{q^* E \epsilon_0 \epsilon_1} \exp\left(-\frac{E}{kT}\right)\right] \quad (2.10)$$

where, K is a constant, σ_0 is the material conductivity, ϵ_0 and ϵ_1 is the absolute and relative permittivity, $q^* = -d/dT(1/T)$. Eqn. 2.10 is expected similar to that derived from the dipolar theory. Eqn. (2.10) shows that a space charge TSDC peak must depend on the nature of the dielectric - electrode interface and predicts a decrease of the current density with decreasing thickness. In dielectric polarized by photoelectric effect or charge injection, the long life time of carriers are assumed to result charge peaks observed in TSDC are usually interpreted in terms of trap limited currents.

The basic equations needed for describing a thermal release from traps are similar to those of the charge motion model except that the density of trapped charge must be introduced as an additional variable while recombination replaces intrinsic conduction as a neutralization process.

During the study of depolarization by the TSDC, the decay of space charge affects carrier drift as well as diffusion. To avoid this an insulating electrode adjacent to the nonmetallized side of the sample (insulating foil or air gap) is used. Since the insulating electrode blocks any charge exchange, all image charges previously induced at the non contacting electrode will be released during the TSDC run and it will be possible to observe the decay resulting from intrinsic conduction.

2.3.4 TSDC involving Interfacial Processes

When structurally heterogeneous materials are investigated, a field induced ionic polarization will obey more closely interfacial model of Maxwell-Wagner-Sillars type.

A simplified TSDC theory of interfacial polarization has been proposed by Harasta and Thurzo [2.6] and Van Turnhout [2.7,8] by considering the model of a charged two layer condenser and neglecting the possible dependence of the permittivities of the two layers on temperature. The expression for the current density is then obtained as [2.6].

$$J_D(T) = \frac{[\epsilon_1\sigma_2(T) - \epsilon_2\sigma_1(T)][\epsilon_2\sigma_1(T_p) - \epsilon_1\sigma_2(T_p)]d_1d_2}{(\epsilon_1d_2 + \epsilon_2d_1)^2[\sigma_1(T_p)d_2 + \sigma_2(T_p)d_1]} V_p \exp\left[-\int_0^T \frac{dT}{q\tau^*(T)}\right] \quad (2.11)$$

where the subscripts 1 and 2 refer to the two layers and $\tau^*(T)$ is relaxation time.

Current is seen to depend on two varying parameters σ_1 and σ_2 and different activation energies E_1 and E_2 will usually be represented by one asymmetrical TSDC peak, the maximum of which is determined by the expression.

$$T_m = \left\{ \frac{\epsilon_0 q (\epsilon_1 d_2 + \epsilon_2 d_1) [\epsilon_1 \sigma_2(T_m) E_2 - \epsilon_2 \sigma_1(T_m) E_1]}{k [\sigma_1(T_m) d_2 + \sigma_2(T_m) d_1] [\epsilon_1 \sigma_2(T_m) - \epsilon_2 \sigma_1(T_m)]} \right\}^{\frac{1}{2}} \quad (2.12)$$

allowing to predict a small shift of the peak with varying thickness of the layers.

2.3.5 The equivalent frequency of TSDC measurements

The equivalent frequency of TSDC measurements i.e., the frequency at which an a.c. experiment should be performed in order to obtain a loss peak having the same maximal temperature as the TSDC peak, can be estimated by relating the heating rate Q and the a.c. angular frequency $\omega = 1/\tau$ via the equation that defines the maximal temperature of the TSDC peak [2.9]

For an Arrhenius shift involving a constant activation energy, the equivalent frequency takes the form,

$$f_{eq} = \frac{\omega}{2\pi} = \frac{1}{2\pi} \frac{qE}{kT_m^2} \quad (2.13)$$

Adopting typical values of the TSDC parameters q , E , T_m this equation leads to $f_{eq} \simeq 10^{-4}$ to 10^{-1} Hz i.e. frequencies which are much lower than those which are able to use under normal conditions in a.c. measurements.

2.6 UV-Visible optical absorption spectroscopy

Electromagnetic radiation of suitable frequency can be passed through a sample so that the photons are absorbed by the samples and changes in the electronic energies of the molecules can be brought about. So it is possible to effect the changes in a particular type of molecular energy using appropriate frequency of the incident radiation.

A display or graph of the intensity of ultraviolet visible (UV-VIS) radiation emitted or absorbed by material as a function of wavelength ranging from 100-400-800 nm is called UV-VIS spectrum and the absorption spectroscopy involving electromagnetic wavelengths in the range 100-400-800 nm is called UV-VIS spectroscopy [2.10].

Representing I_0 and I_t as the Intensity of the incident and transmitted light the absorption law is given

$$I_t = I_0 \exp(- \epsilon cl) \quad (2.14)$$

Which shows the intensity of the emitted light decreases exponentially as the thickness and concentration of the absorbing medium. Here l is the path length of the absorbing material and c is the concentration and ϵ = molecular extinction coefficient.

The absorbance or optical density is defined as the logarithmic ratio between the intensities of the incident and transmitted radiations.

$$Absorbance = \log_{10} \frac{I_0}{I_t} \quad (2.15)$$

From eqn. (2.14) and (2.15) one can get

$$Absorbance = \log_{10} \frac{I_0}{I_t} = \epsilon cl \quad (2.16)$$

This equation is the fundamental equation of spectrophotometry and is often spoken of as the Beer - Lambert Law. The outer-shell electrons are absorbed into the UV and visible region because they are loosely bound to the nucleus.

Ultraviolet and visible spectroscopy finds application in the identification of a compound. The identity of a synthetic product generally of its spectrum is compared with that of the natural product or another standard sample. It is a powerful method of impurity detection. UV-Visible spectroscopic methods are widely used for the quantitative determination of substances, determination of molecular weight, structure, diagnosis, study of equilibrium in solutions.

2.5 Literature review

S.N. Maiti and P.K. Mahapatro[2.11] studied crystallization of isotactic polypropylene (i-PP) in the i-PP/Aluminum composites through differential scanning calorimetry (DSC) and wide angle X-ray diffraction measurements. Crystallization of i-PP in i-PP/Al powder Composites was estimated from the crystallization exotherm of i-PP in DSC thermograms of the composites. In the region of low filler volume percent (0-3.5%) Crystallinity decreases which induces reduction in tensile strength, modulus and elongation. Crystallinity decreases further upto 1.7 volume percent filler and it then exhibits a small increase up to 3.3% filler. Tensile strength, modulus, and elongation at yield show almost steady decrease at these filler concentrations. Finally in region of filler content 3.3 -10.5 the crystallinity slowly decreases. The corresponding decrease in tensile strength, modulus and elongation is also very slow. Tensile strength, tensile modulus and elongation at yield are predominately dependent on the crystallinity of i-PP in the composites.

M. Sova et al.[2.12] studied the low temperature impact behaviour of PP composite materials oriented by solid state drawing method. Isotactic polypropylene samples, both neat and containing short glass fibers, with two different interfacial adhesions, were oriented by solid state drawing with typical neck propagation. Unidirectional composite materials can be prepared from injection molded polypropylene samples containing short glass fibers via solid-state drawing. Extensive movements of fibers, accompanied by the transformation of PP crystalline structure support the concept of strain-induced "melting" of the polymeric matrix in the neck shoulder. Oriented i-PP composite materials possess high toughness down to liquid nitrogen temperature, if the main crack propagate across the drawing direction. The properties of the interesting class of polymeric composite materials prepared by solid state drawing can be further optimized by varying interfacial adhesion, drawing conditions and subsequent treatment.

George R. Lightsay et al.[2.13] studied the effect of surface chemistry of cellulosic fillers on the properties of PP composites. Cellulosic fillers such as wood flour have both low specific gravity and low cost and have been used as extenders in thermosetting polymers for many years. Cellulosic fillers with different polymers surface characteristics were evaluated in PP. The fillers were mixed at various concentrations (fur loading) with Hercules 7401 PP powder and then dried at 110⁰C for 30 minute just prior to molding. Tensile, flexure and impact samples were molded using an injection molder. The more polar nature of wood flour and pulp mill fines in comparison to thermomechanical pulp explain why composites containing thermomechanical pulp were generally superior composites containing either wood flour or pulp mill fines. The improvements noted in composites containing wood flour or pulp mill fines that had been coated with a nonpolar resin indicates that it is the surface of the filler polymer bonding. Coating of cellulosic fillers with non polar resin is usually expensive.

R.Nath and M.M.Perlman[2.14] studied the effect of crystallinity on PP and PE. Charge storage is greatly improved by annealing, different cooling rates, and stretching in PP and PE. In annealed PP and PE storage increases linearly with both crystallinity and crystallite size. The half value charge decay temperature can be used as a measure of the later parameter. Annealing and cooling rate affect the rate of crystalline growth. Changes occur in both the physical and / or chemical nature and concentration of defects in the crystalline region or traps at chain fold- amorphous interface. Annealing 4:1 stretched PP film at 140⁰C gave a half value charge decay temperature of 152⁰C ~ 70⁰C higher than unannealed unstretched film. Stretching increases amorphous content creating new boundaries, decreases crystalline size and creates defect traps.

Newspaper fiber-Reinforced polypropylene composite was made by Shan Ren and David N.S. Hons[2.15]. A method of applying newspaper sheet directly to polypropylene without any treatment was developed. Experimental results revealed that, the composites made from this method were twice as strong as the polypropylene without newspaper. Composites of newspaper fiber (NPF) and polypropylene (PP) can be made through an

intensive mixing process. It was found that newspaper can be fed into the mixer directly, without defibration, in the presence of water. In addition to newspaper fiber, corrugated board were also found to have a reinforcing effect on the composites.

P. Karanja and R.Nath[2.16] studied the charge trapping and conduction in pure and iodine doped biaxially oriented polypropylene (BOPP). Structural and chemical modification were investigated using X-ray, optical and infrared methods. Optical spectra of doped BOPP show absorption at 290 nm from charge transfer complexes. X-ray examination revealed a decreases in crystallinity and crystallite size after doping. Effect of iodine on charge trapping was determined by TSDC technique. Deep traps (120^oC peak) at crystalline amorphous interfaces are destroyed by iodine which provides new traps (68^oC peak) with activation energy 0.9 ev. Pressure dependence of conductivity indicates ionic conduction in pure samples and electronic conduction in doped samples. It was proposed that trapped electrons (arising due to donor-acceptor action) are thermally released through PF lowering, predominately contribute to the conduction.

Character of crystallization nuclei in i-PP was studied by Frantisek Rybnikar[2.17]. Examination of the isothermal crystallization and the effect of melting conditions on samples of isotactic polypropylene and its composite with Talc, combined with electron microscopic observation shows two types of heterogeneous nuclei effective in the crystallization process. The study of the crystallization behaviour of i-PP at various T_c values and of the effect of melting conditions on the crystallization nuclei number, together with electron microscopy, disclosed information on the character of the heterogeneous nuclei active in the bulk crystallization of i-PP from the melt. Depending on the melting conditions, two kinds of heterogeneous nuclei initiate the crystallization. At low melting temperatures and / or short melting periods, the metastable nuclei dominates, representing the remnants of the polymer crystalline phase, stabilized above T_m by the action of heterogenities. The second kind of stable heterogeneous nuclei is most probably associated with the nucleation substrate, characterized by a lamellar structure with overall dimensions in the order of several microns. It was assumed that the

nucleation substrate represents essentially residues of polymerization catalysts. The character of the interaction of *i*-PP with the nucleation substrate lies between crystallization on the substrate surface steps and epitaxial crystallization, similarly to what was established in polyolefins filled with Talc.

The electrical properties i.e volume resistivity, dielectric permittivity and dielectric loss factor as well as thermally stimulated depolarization current (TSDC) were measured on polypropylene (PP)- polycarbonate blends by P. Myslinski et al.[2.18]. The results confirmed the existence of some interactions between the non compatible components of PP-PC blends. It is observed that the volume resistivity varies proportionally to the blend composition. Dielectric loss factor versus temperature in the range of 20-105°C are represented by similar curves for each blends Dielectric loss factor has sharply increased above 130°C as for pure PC, and should reach the maximum at glass transition temperature T_g of PC i.e. at above 150°C. The maximum at 150°C was, however not found. Thus the continuous increase of $\tan \delta$ should be attributed not only to the relaxation of polar groups in PC, but also to the relaxation of free charges in the blends. TSD current for PP-PC blends depend above all on the PC content, and two maximum of current intensity are observed : the higher intensity maximum is at about 150°C. The Second which could be connected with the presence of PP in the blends and attributed to the melting temperature of PP. The maximum at 65°C typical of pure PP, is not observed for PP-PC blends.

Applying thermally stimulated depolarization current method, anelastic and dielectric properties of Polyether-Polyamide copolymer have been studied by H.S. Faruq and C. Lacabane[2.19]. They have observed that the relaxation peaks resulting from molecular motions are similar to those observed in homopolymers. The mechanical properties depend primarily on the hard segment constant. The domain morphology is effected by thermal treatment. The same authors have studied the phase segregation in poly (ether block amide) co-polymer by thermally stimulated depolarization (TSD). Well defined, complex and partial phase segregation were observed depending on the molecular mass of each

segment of the copolymer. A new glass transition peak appeared when transitions were observed. Soft segment component poly tetramethylene glycol (PTMG) with a lower molecular mass, was found to be completely amorphous. No additional Maxwell - Wagner - Sillers (MWS) effect at the phase boundaries was detected.

Creep behaviour of biaxially - rolled PP was studied by J.X. Li and W.L. Cheung[2.20]. PP was biaxially rolled up to 60% at ambient temperature and the tensile creep behaviour over the temperature range 27 to 60⁰C was investigated using a dead load apparatus. The degrees of crystallinity of the as - molded and rolled PP were determined using a differential scanning calorimeter (DSC) and density bottle. The DSC shown a slight change in the crystallinity during the early stage of the rolling process, while the density bottle indicates a continuous drop of the density with increasing rolling reduction. The elongation due to rolling was found almost fully recoverable when the samples were thrown into hot silicon oil at 180⁰C. The effects of cold rolling on creep strain, secondary creep strain rate, and creep activation energy were investigated. Cold rolling led to an increase in the creep stain and secondary creep strain rate. The creep activation energy was found to increase with increasing rolling reduction. Within the secondary creep stage, the creep process in PP is mainly due to α -relaxation process and most of the creep strain was recoverable.

M. Gahleitner et al.[2.21] presented a comparative study of rheological and mechanical properties of PP compounds with Talc as a mineral filler. It turns out that the main factors determining the mechanical behaviour, namely (a) filler concentration, (b) filler particle size, and c) degree of dissipation, influence the linear viscoelastice properties as well. The determination of linear viscolastic properties of a mineral filled thermoplastic material in the melt provide a quick and reliable way to investigate filler properties and dispersion quality.

References of chapter - II

- 2.1 A. Servini and A.K. Jonscher, *Thin Solid Films* 3 (1969) 341.
- 2.2 C. Bucci and R. Fieschi, *Phys. Rev Lett.* 12 (1964) 16.
- 2.3 Chen, R., *J.Mater. Sci.* 11 (1976) 1521.
- 2.4 P. Muller, *Phys. Status Solidi A*23 (1974) 165.
- 2.5 G.F J. Garlick and A.F.Gibson, *Proc. Phys. Soc. London A*60 (1948) 574.
- 2.6 V.Harasta and I. Thurzo, *Fyz. Casop. (Czech)*, 20(1970) 148.
- 2.7 J.Van Turnhout, *Polym. J.* 2 (1971) 173.
- 2.8 J.Van Turnhout, *Thermally Stimulated Discharge of Polymer Electrets* (Elsevier, Amsterdam, 1975).
- 2.9 M. Abkowitz, P..J.Luca, G.Pfister and W.M.Prest. Jr: *Proc.Piezoelectric and Pyroelectric Symposium - Workshop* (Nat. Bur. Stand. U.S., Interagency Report, NBSIR, 75-760 (1975) 96-119.
- 2.10 Sybil P. Parker, "Mc Graw Hill Dictionary of Physics" 1986.
- 2.11 S.N. Maiti and P.K.Mahapatro, *J. Polym. Mater.* 6 (1989) 107-14.
- 2.12 M.Sova, M. Raab and M Shzoba, *J. Mater. Sci.* 28 (1993) 6516-6523.

- 2.13 George R.Lightsay, Paul H.Short, Kathryn S. Kalasinsky and Logan Mann, J. Miss. Acad. Sci. (USA) 24 (1979) 76-86.
- 2.14 R. Nath and M.M. Perlman, IEEE Trans. Electr. Insul. 24 (1989) 1311-1322.
- 2.15 Shan Ren and David N.S. Hons, J. REINFORCED PLASTICS AND COMPOSITES 12 (1993) 1311-1322.
- 2.16 P. Karanja and R. Nath, IEEE Trans. Dielectr. Insul. 2 (1994) 213 - 223.
- 2.17 Frantisek Rybnikar, J.Appl. Polym. Sci. 27 (1982) 1479-1486.
- 2.18 P. Myslinski, Z. Dobkowski and B.Krajewski, "Polymer Blends Processing. Morphology and Properties" 2 Eds. E. Martus Celli, R. Palumbo and M. Kryszewski. Plenum Press NY, London (1984) 157 - 163.
- 2.19 H.S. Faruque and C. Lacabenne, J. Phys. D : Appl. Phys. 20 (1987) 939-944.
- 2.20 J.X.Ji and W.Z. Cheung, J. Appl. Polym. Sci. 56 (1995) 881-888.
- 2.21 M. Gahleitner, K.Bernlitner and W.Neible, J. Appl. Polym. Sci. 53 (1994) 283 - 289.

CHAPTER-III

EXPERIMENTAL DETAILS

- 3.1 Raw materials used in this research work
- 3.2 Details of the fabricated extrusion machine set up in the laboratory
- 3.3 Preparation of the different samples
- 3.4 Electrode deposition
- 3.5 UV-Visible optical absorption spectroscopy
- 3.6 Instruments used in TSDC measurements
- 3.7 TSDC measurements
 - 3.7.1 General procedure for TSDC measurements
 - 3.7.2 The present TSDC measurements

Chapter - III

Experimental Details

3.1 Raw materials used in this research work

Composites used in this research work were prepared from Polypropylene (PP) and Hydrous Magnesium Silicate (Talc). Composites were prepared in different mixing ratios. Details of the origin and physical properties of the raw materials used in this study are given below.

a) Polypropylene

Polypropylene (Novolen 1100L 2510025) was obtained from BASF, Germany in the form of solid pieces.

- i) Melting temperature, $T_m = 338\text{K}$
- ii) Refractive index $\mu = 1.3567$
- iii) Glass transition temperature, $T_g = 270\text{K}$

b) Hydrous Magnesium Silicate (Talc)

It was obtained from Konoshima Chemical Co. Ltd., Osaka, Japan and was in the powder form. It is soluble in hot concentrated phosphoric acid.

- i) Density = 450 Kg/m^3
- ii) Melting temperature, $T_m = 1073\text{K}$

3.2 Details of the fabricated extrusion machine set up in the laboratory

Extrusion is the process of pushing the heated billet or slug of polymers, composites etc. through an orifice provided into a die, thus forming an elongated part of the uniform cross-section corresponding to the shape of the die orifice. It is a faster process. The products have good tolerances and have good surface finish. Complex shapes can be easily extruded.

The various parts of the fabricated extrusion machine (Fig. 3.1) set up in the laboratory are described below.

1. The extruder screw

The most important element of the extrusion machine is the extrusion screw. This delivers material through the die. The length of the screw is divided into three zones: feed, compression and metering. The purpose of feed zone is to pick up the mixed batch of PP and Talc from the feed hopper and to move them into the main length of the extruder. In the compression zone the loosely packed mixture is compacted and softened to produce a continuous stream of molten composite from the compression zone and feeds it at a controlled rate through the die.

The screw is driven by an alternating current motor. Continuous variation of screw speed is normally required. A screw of smaller diameter must be operated at a faster speed than one of the larger diameter. Speeds of operation range will be below 100 rpm to above 100 rpm.

The fabricated extrusion machine set up in the laboratory has the following specifications for the extruder screw.

- i. Length of screw = 0.80 meter
- ii. Length between turns of screw = 0.038 meter
- iii. Height of the turns = 0.00635 (starting) meter and 0.00159 meter. (finishing)
- iv. r.p.m. of the screw = 96
- v. Diameter of the screw = 0.045 meter

2. The barrel

The barrel surrounds the screw. It resists the pressure generated by the screw, which may be as high as 6000 psi. Cold water is circulated around the barrel at the feed hopper side to prevent the plastic granules from sintering together and thus blocking the feed opening. Usually, the length of the barrel was electrically heated by band heaters around it. A polymer heated to an excessive temperature could degrade. The cooling system may use water in copper tubes, room or supplied by fan or other means.

The fabricated extrusion machine set up in the laboratory has the following specifications for the barrel.

- i. Length of the barrel = 0.082 meter.
- ii. Inner diameter = 0.012 meter.
- iii. Outer diameter = 0.0135 meter.

3. Profile dies

Dies for profiles such as moldings, counter edging, rods etc. have an orifice of the approximate shape and size of the required contour, the final shape developing outside the die as the material wraps and shrinks or expands. By trial on the extruder the shape of the die orifice is modified as required. The size and shape of an extended profile can also be changed by altering the extrusion speed and the rate of cooling after the composite leaves the die. Usually the die orifice is made oversize.

4. Cooling and take off equipment

As the fluid composite leaves the die, it must be supported by a shaping fixture usually called a sizing plate, to retain the desired shape through the period when the material cools. By changing the speed of the take off equipment it is possible to control the dimension of the contour; a faster take off will produce greater draw down.

5. Breaker and screen pack

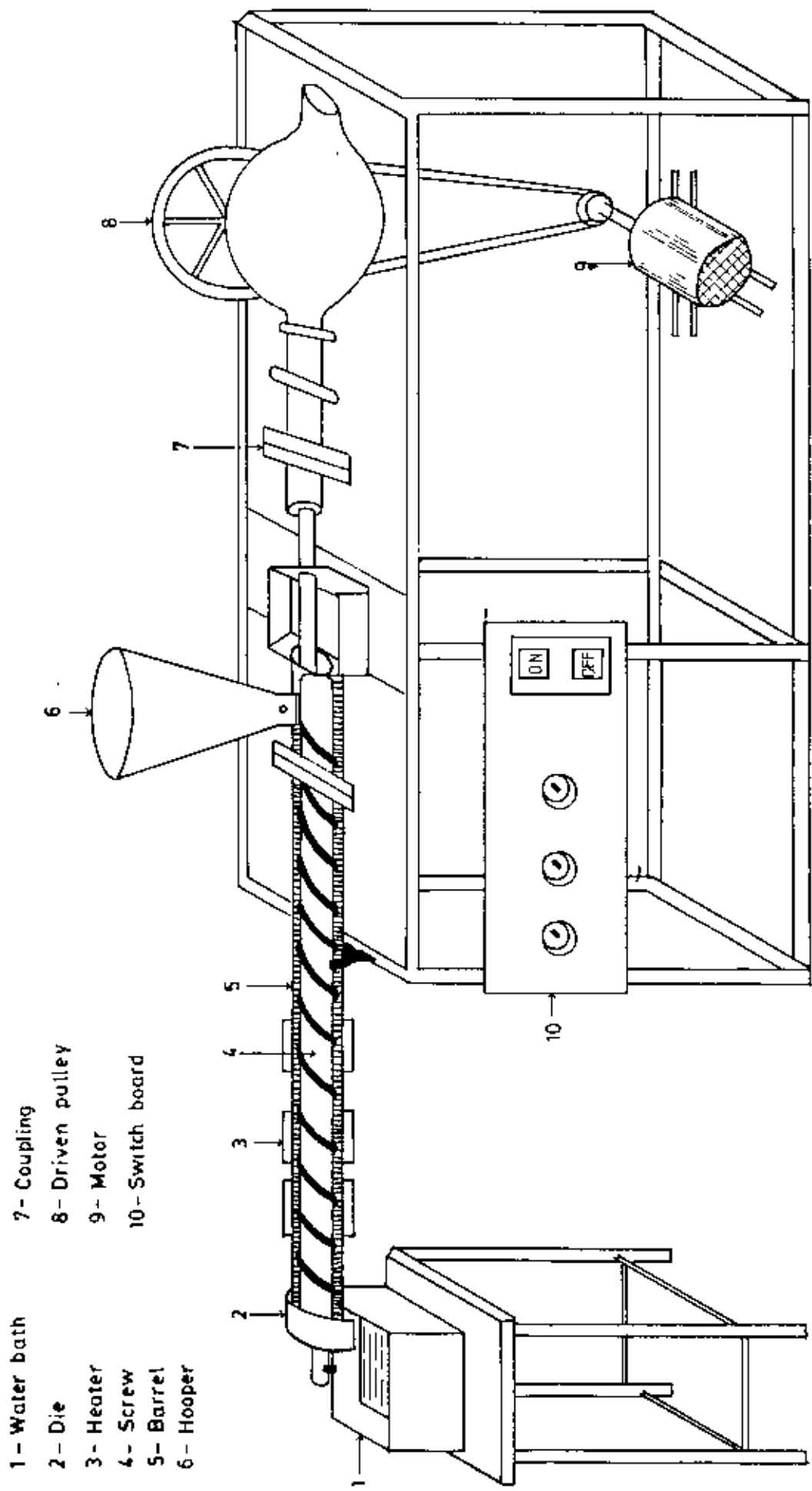
At the end of the screw the plastic is delivered through a breaker plate and screens to the die. The breaker plate is a thick plate drilled with holes about 1/8 to 1/4 inch in diameter. The screen pack consists of several layers of stainless wire screen which strain out foreign material and unmelted granular substances.

6. Heaters

The fabricated machine has three heaters situated at a distance of 0.09 meter from each other. The heaters can heat the barrel up to 513K.

7. Motor

A motor (5 HP, 1440 rpm) was incorporated to the extrusion machine. The diameter of the motor pulley is 0.3048 meter and driven pulley is 0.1016 meter.



- 1 - Water bath
- 2 - Die
- 3 - Heater
- 4 - Screw
- 5 - Barrel
- 6 - Hooper
- 7 - Coupling
- 8 - Driven pulley
- 9 - Motor
- 10 - Switch board

Fig. 3-1: Fabricated extrusion machine set up in the laboratory

3.3. Preparation of the different samples

Samples with different composition ratios of PP and Talc were prepared by the following way. At first, five batches of different mixing ratios were made with PP and Talc according to the following formula.

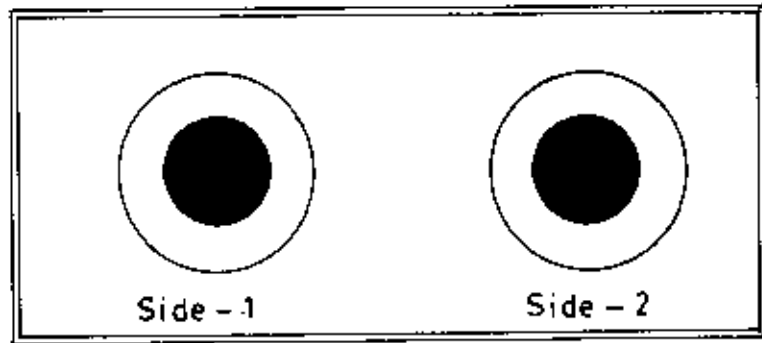
$$(10-X) \text{ PP} : X \text{ Talc} \quad | \quad X = 1,2,3,4,5,$$

Besides these a pure Polypropylene sample was also prepared.

The mixtures were put into separate pot and then mixed uniformly as much as possible. The different mixtures were melt by extrusion technique. Initially the three heaters of the extrusion machine were switched "ON" for about one hour. When the barrel temperature was reached to a temperature of about 513K, the mixture was put into the feed hopper. The motor was then switched "ON" to send the batch from the feed hopper into the barrel through the feed zone. The material was then melted during passing through the compression and metering zone and the molten material was then collected through die in the form of rod. The rods were cooled in a water bath during collection. The rods were then cut with a hexsaw to pellets. The surfaces were polished. Thus the disc shape specimens of composite pellets of different thickness were obtained. Then these were pressed using a hydraulic machine to a pressure of 5000 PSI at 398K for five minutes.

3.4 Electrode deposition

The samples were stored in a desicator for one week. Then silver dag (Ledinings silver D200, DEMEIRON, Germany) was applied to each of the first circular surface. The silver dag coated area on both the surfaces of a sample were equal. Here silver dag acts as conducting metallic coating. These coatings served as electrodes for TSDC measurements.



The Specimen

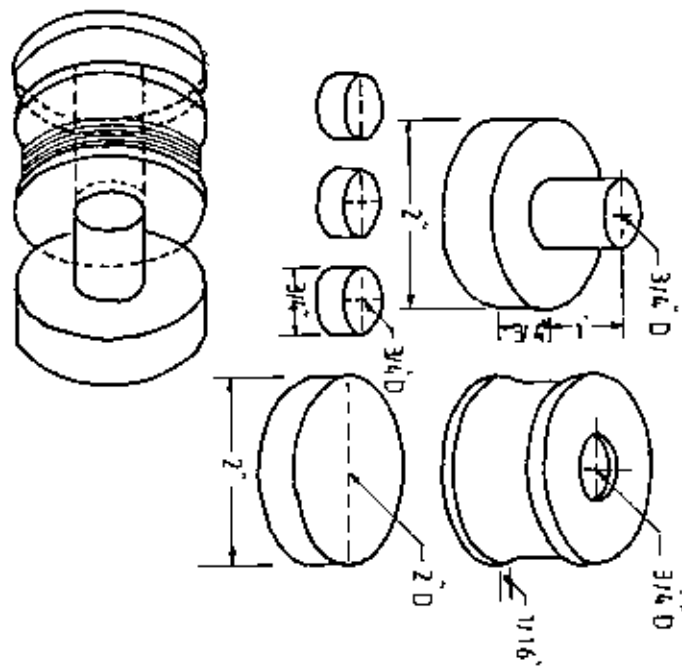


Fig. 3.2 Schematic diagram of the Die .

3.5 UV - Visible optical absorption spectroscopy

The UV - visible optical absorption spectra of different samples were recorded at room temperature using an UV-visible recording spectrometer UV-160A of Shimadzu Corporation, Japan.

3.6 Instruments used in TSDC Measurements

(a) Keithley 614 Electrometer

A digital Keithley Electrometer (model 614, Keithley Instrument Inc, Cleveland, Ohio, U.S.A) was used for D.C current measurement. It is a very sophisticated instrument and it has a versatile uses. It can measure a wide range of d.c voltages, currents, resistance, and electric charge. Resistance range of this model is from 1 ohm to 2×10^{11} ohms using the constant current technique. This electrometer can measure current as low as 10^{-14} A. Voltage range is 10 μ V to 20V with an input impedance of greater than 5×10^{13} ohms. It has an analog output of 2V.

(b) D.C Power Supply

A high voltage d.c power supply was used which was designed and fabricated from Bitek engineering workshop, Dhaka. This unit is capable of supplying d.c. voltages from 0 to 600 volts with a current range from 0 to 100 mA.

(c) Oil Rotary Pump

An oil rotary pump (VS35A) was used to evacuate the specimen chamber. A pressure of about 10^{-2} torr can be attained using this pump.

(d) Specimen Chamber

Specimen chamber shown in Fig. 3.3 is designed and fabricated in the laboratory with the help of the university workshop. This unit basically consists of two main parts, mainly, the stainless steel tube and the sample holder

A stainless steel tube having inner diameter of 0.045 m and length 0.24 m is used. The lower end of the tube is closed by welding a circular piece of stainless steel sheet. At the top of the tube one flat stainless steel sheet (0.092 X 0.09 m²) with a circular hole (diameter 0.045 m) at its center is welded. Another stainless steel sheet (same as above) with a hole of the same dimension is welded to a stainless steel tube of diameter 0.045 m and of length 0.24 m. A O-ring is placed in between the two stainless steel sheets. This prevents the air leakage when it is evacuated. The upper portion can be fixed to the lower portion by screws. The top opening is closed tightly with a teflon stopper. Two copper leads (electrodes) which hold the specimen holder and a Chromel-Alumel (Cr-Al) thermocouple is inserted through this teflon stopper. A thick layer of mica sheet is placed on to the inside wall and bottom of the stainless steel tube for electrical insulation. The distance between the leads is about 0.014 m. There is a side tube welded to the main stainless steel tube which acts as an outlet of the chamber. A rotary vacuum pump is connected to the chamber through the side tube with the help of rubber tube. By this pump a pressure of about 10⁻² torr can be obtained. Required temperature in the chamber can be maintained by a heating tape which is wrapped outside the tube and its temperature is controlled by a variable transformer. Sample holder is a spring system.

(e) Heating Tape

A heating tape (ISOPAD LTD BOREHAMWOOD, HERTS, ENGLAND) was used to heat the specimen chamber. It is about 1.75 m long and 0.03 m width tape. It can be wrapped around the specimen chamber easily.

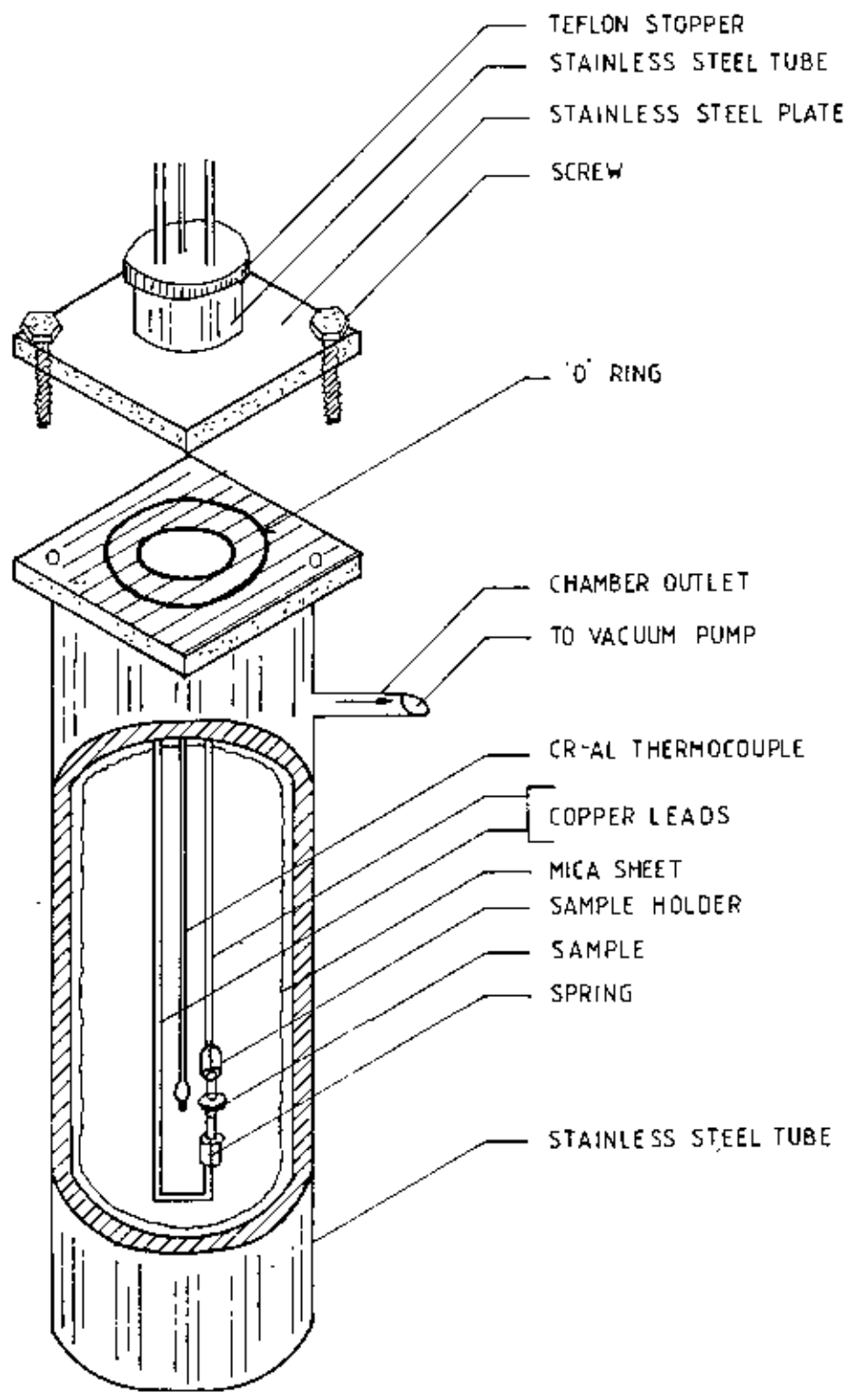


Fig. 3.3: The schematic diagram of the specimen chamber.

(f) Pen recorder

A Shimadzu XY-50 pen recorder was used to record the TSDC spectrum. The analog output of the digital electrometer was connected to the input of the recorder.

(g) Variac

A Yamabishi volt - slider (Type SS - 260 - 10 No. 38 - 1) was connected to the heating tape.

3.7 TSDC MEASUREMENTS

3.7.1 General procedure for TSDC measurements

The general procedure for TSDC measurement is described below. The specimen was first polarized with a d.c. field E_p at temperature T_p for a time t_p . Here T_p is called polarizing temperature, E_p is called polarizing field and t_p is called polarizing time. T_p should be high enough for dipole alignment but low enough to avoid significant space-charge polarization. The specimen with E_p still applied, is quenched to a low temperature $T_0 \ll T_p$, where dipole motion is essentially negligible. At T_0 , E_p was removed, the two electrodes are temporarily short circuited for certain period of time and the specimen was connected to an electrometer. As the specimen was heated at a constant rate, the discharge current was recorded as function of temperature by a pen recorder

3.7.2 The present TSDC measurements

At first the specimen was placed in between the electrodes. The specimen chamber was evacuated to about 10^{-2} torr by a rotary pump. Then the temperature of the specimen was raised to different fixed temperature called polarizing temperature (T_p). After attaining a particular T_p , an electric field was applied across the specimen to polarize it for a period of time called polarizing time $t_p = 15$ min. The specimen was then quenched to a lower temperature $T_0 = 223K$ by immersing the specimen chamber in liquid nitrogen with the field "ON". At T_0 the electric field was removed and the two electrodes were shorted for about 10 min to discharge any excess charge. Then the electrometer was connected to measure the depolarization current

The linear increase of the temperature with time in the chamber was ensured by heating the tape connected to a variable transformer. To maintain constant heating rate, the variac was adjusted manually by increasing or decreasing the applied voltage by the variable

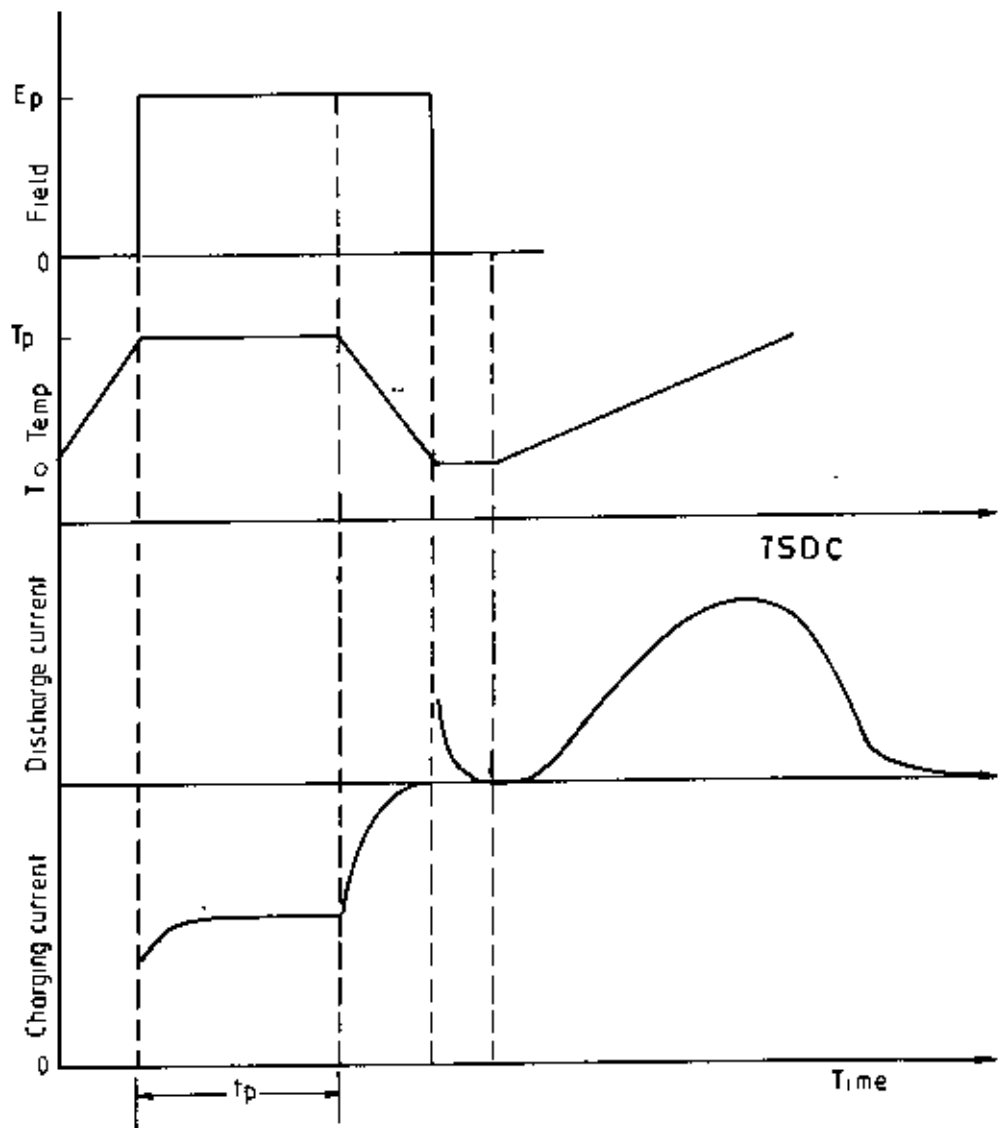


Fig. 3.4 . TSDC Measurement Sequence

transformer which was ensured on practice earlier. The heating rate was maintained to about 3 K/min.

In the present TSDC measurements, each sample was first polarized by a fixed polarizing voltage, $V_p = 500\text{V}$ at various polarizing temperatures, $T_p = 333, 353, 373$ and 393K for polarizing time, $t_p = 15$ min and then polarized by different $V_p = 500, 400, 300$ and 150V at a fixed $T_p = 393\text{K}$ for $t_p = 15$ min.

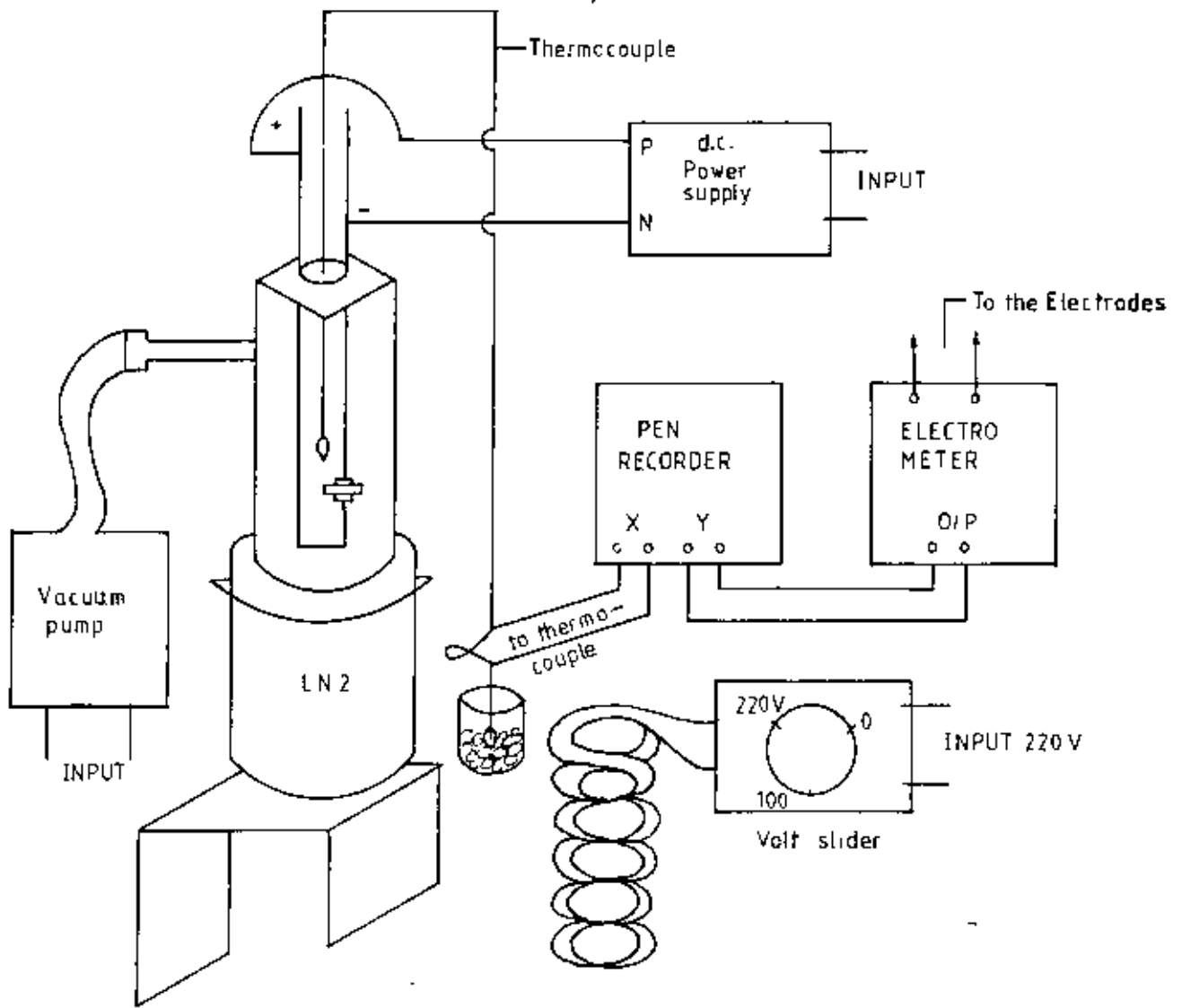


Fig 3.6 TSDC Experimental set up

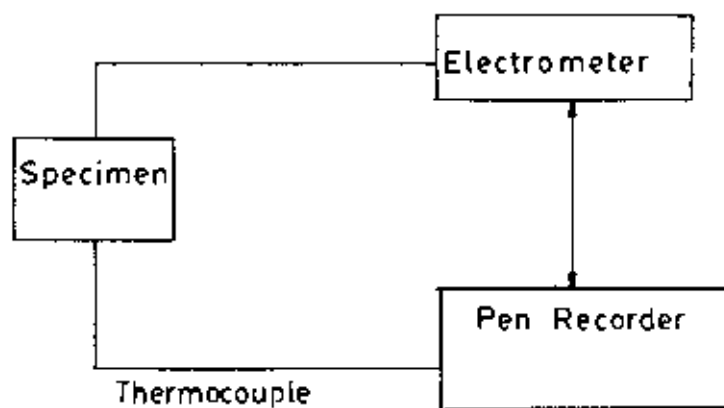
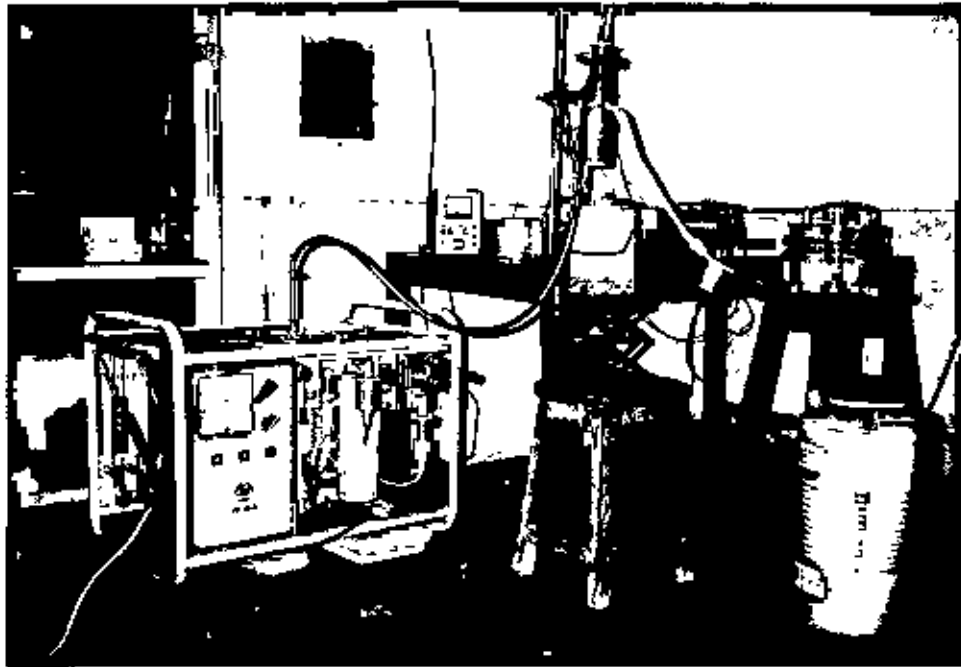
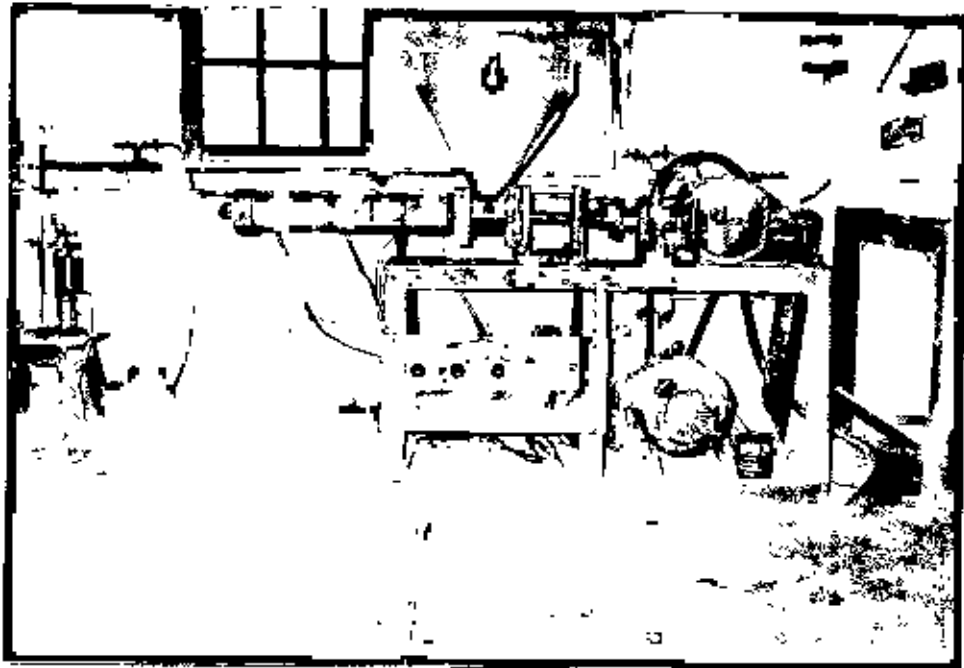


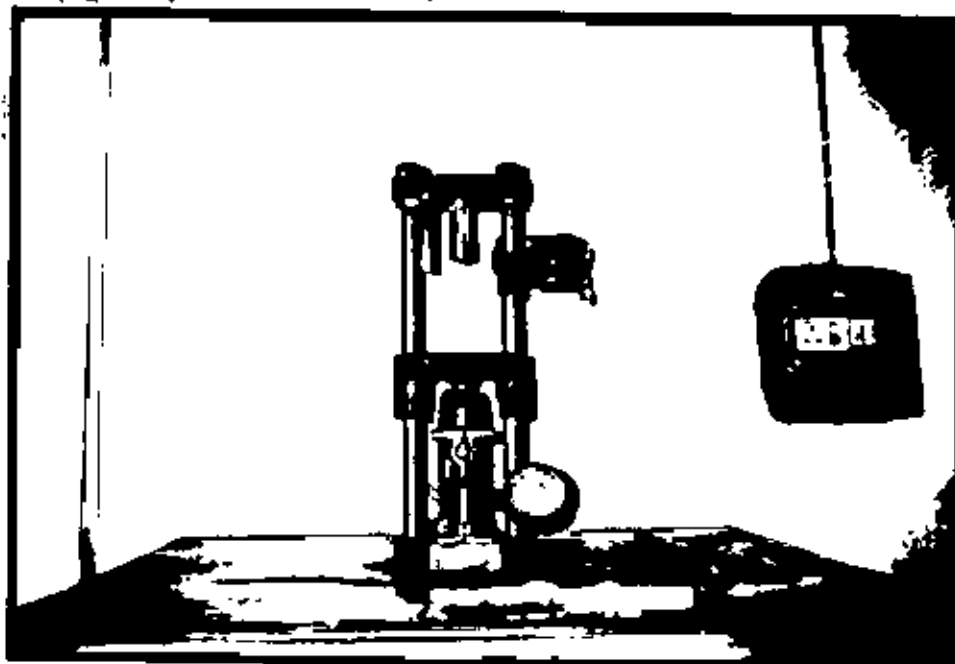
Fig 3.5: Simplified circuit diagram of TSDC measurement.



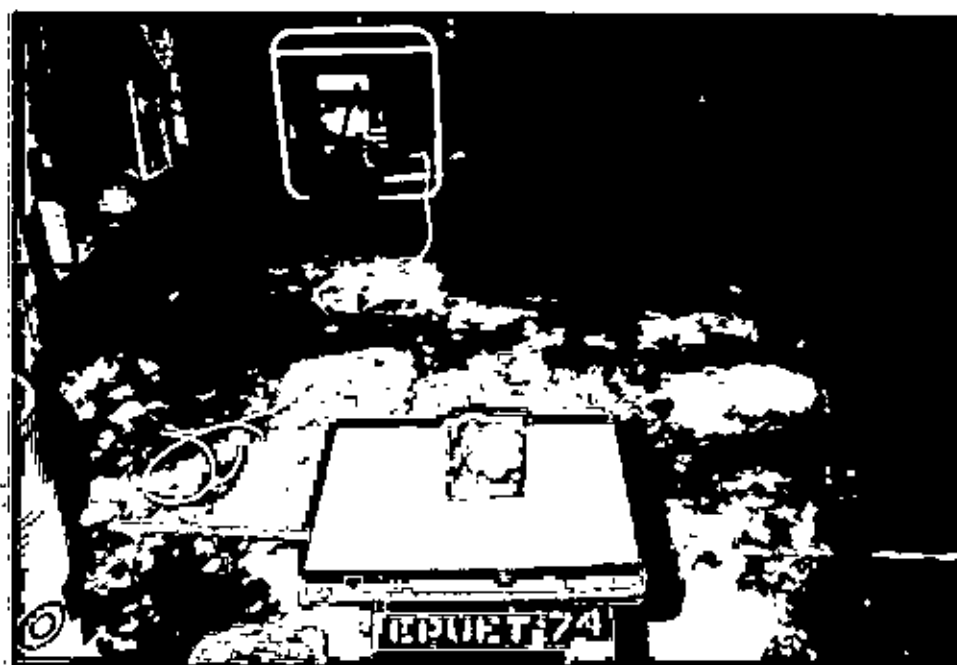
PHOTOGRAPH : TSDC EXPERIMENTAL SETUP



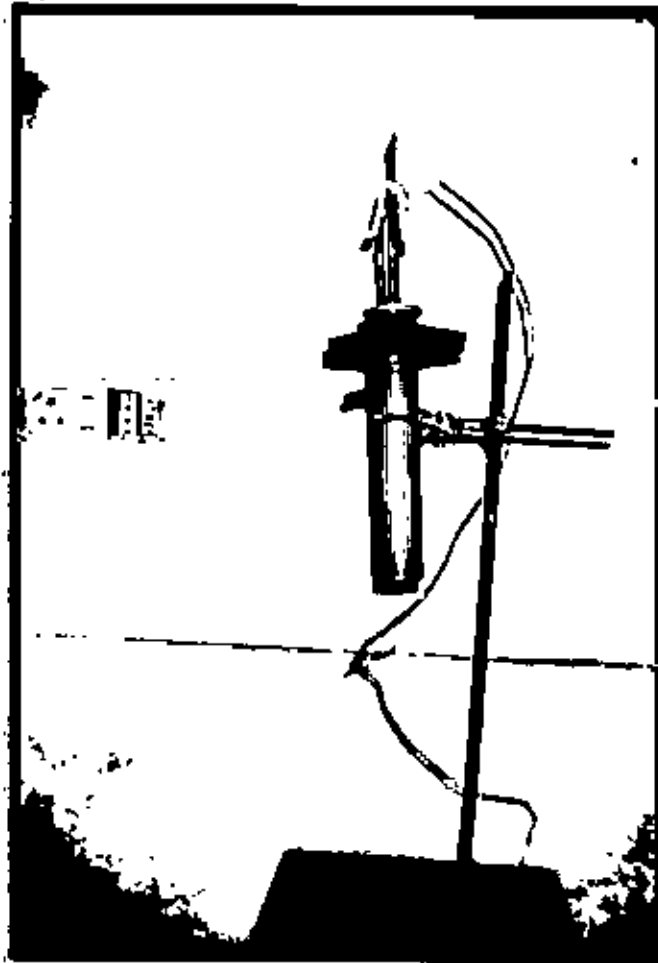
PHOTOGRAPH : THE EXTRUSION MACHINE SET UP IN THE LABORATORY



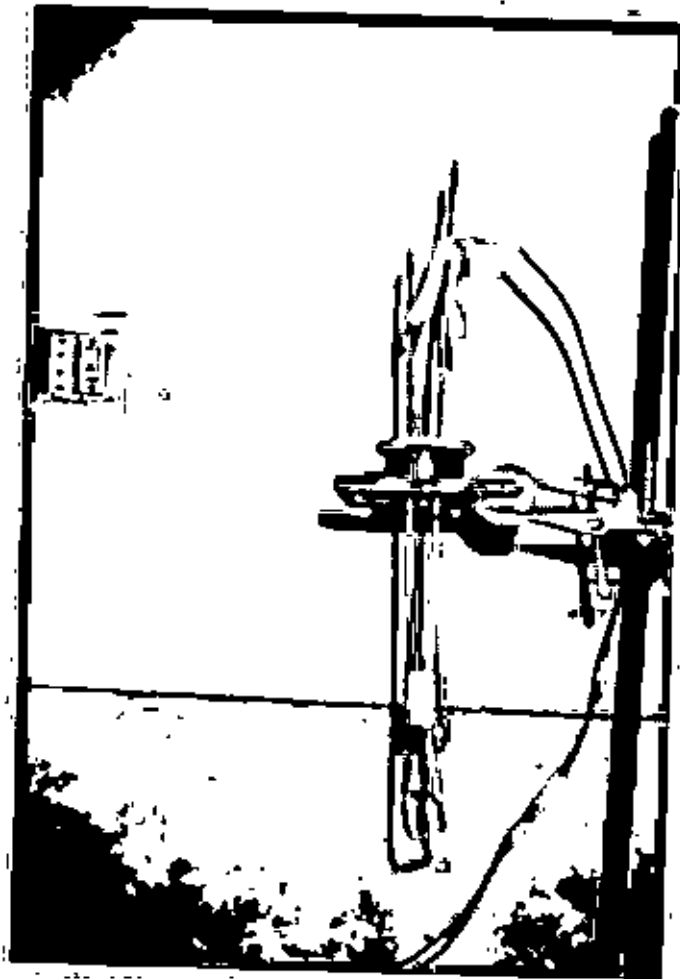
PHOTOGRAPH : THE HYDRAULIC PRESS



PHOTOGRAPH : SAMPLES



PHOTOGRAPH : THE SPECIMEN CHAMBER



PHOTOGRAPH : THE SPECIMEN HOLDER

CHAPTER-IV

RESULTS AND DISCUSSION

- 4.1 UV-Visible optical absorption spectra
- 4.2 Thermally stimulated depolarization current (TSDC) measurements
 - 4.2.1 TSDC spectra for pure PP
 - 4.2.2 TSDC spectra for composites
 - 4.2.3 Dependence of the total charge Q released on the Vp and Talc content (wt%)
 - 4.2.4 Activation energy from TSDC

References

Chapter-IV

Results and discussion

4.1 UV- Visible optical absorption spectra

The room temperature UV- visible absorption spectra of PP and PP-Talc composites with different wt(%) recorded in air in the wavelength ranging from 200 to 800 nm are presented in Fig. 4.1. It is observed that the absorption increases drastically with increasing talc (wt%) throughout the whole wavelength range .

It is observed that there is an absorption minimum around 370-414 nm in the spectra of composites whereas absorption increases monotonically with decreasing wavelength in case of PP . The absorption spectra of PP shows a peak at 275 nm which may be attributed to the possible association of oxygen in the PP matrix during processing . In biaxially oriented PP a weak band has been observed at 390 nm which was attributed to impurities and/or additives [4.1]. Such bands are also seen at about 380-400 nm in the present measurement. There is a band at 300-350 nm which may be due to $n-\pi^*$ and $\pi-\pi^*$ transitions. The absorption coefficient, α , was calculated from the measured optical absorption for PP and PP-Talc composites presented in Fig. 4.1 The spectral dependence of α as a function of $h\nu$ for all the samples are shown in Fig. 4.2. It is seen that the edges do not fall sharply. This indicates that there are defect states within the bandgap. The bandgaps (E_g) determined from the intercept of the line drawn in the high energy side . The values of E_g are depicted in table I. It is seen that the E_g value decreases after adding 10(wt%) Talc in PP and it is not much affected on further addition of Talc in PP.

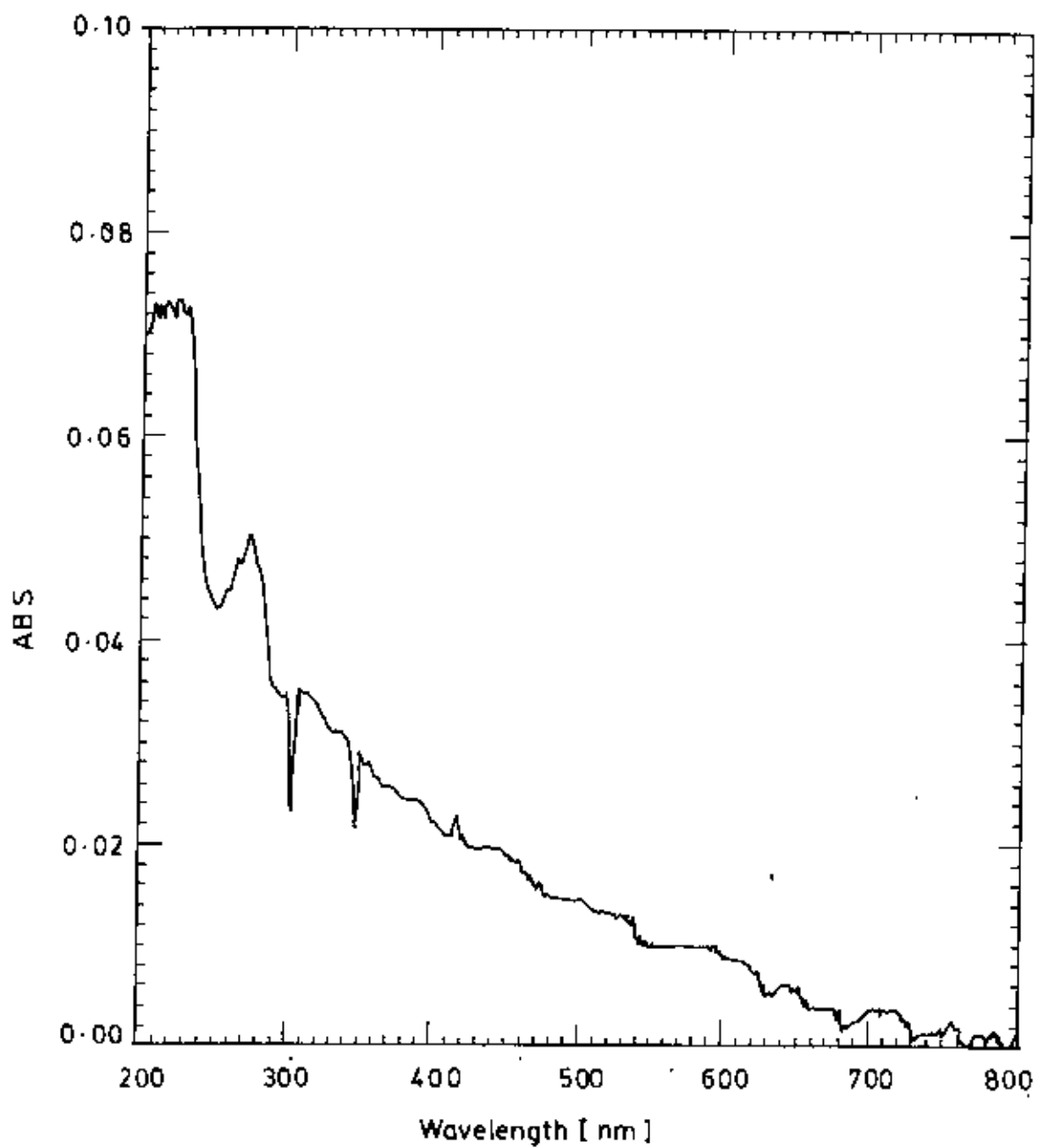


Fig 4.1.a: UV - VIS spectroscopy for sample pure PP

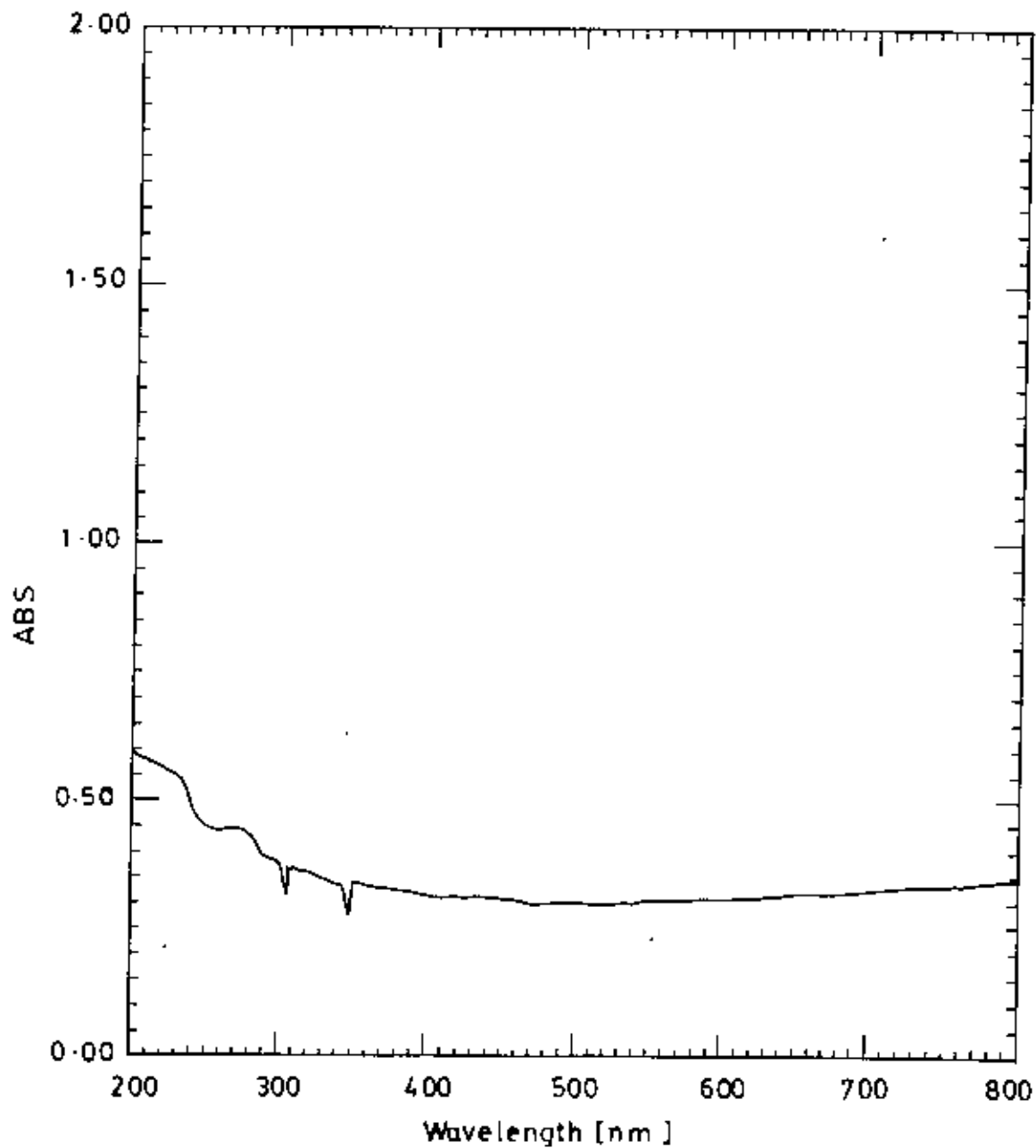


Fig. 4.T.b: UV - VIS spectroscopy for sample PP: Talc = 9:1

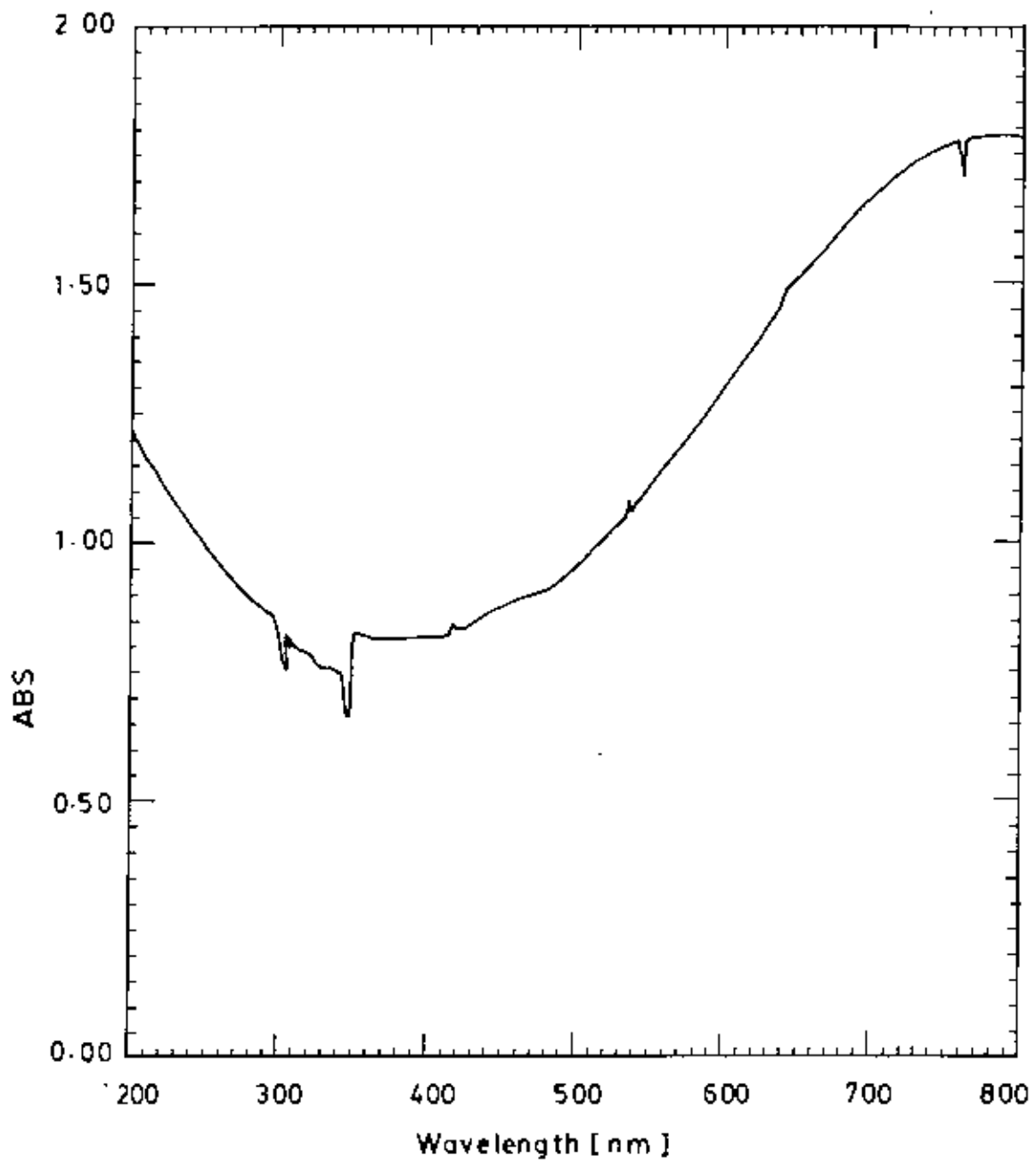


Fig. 4.1.c: UV - VIS spectroscopy for sample PP:Talc = 8:2

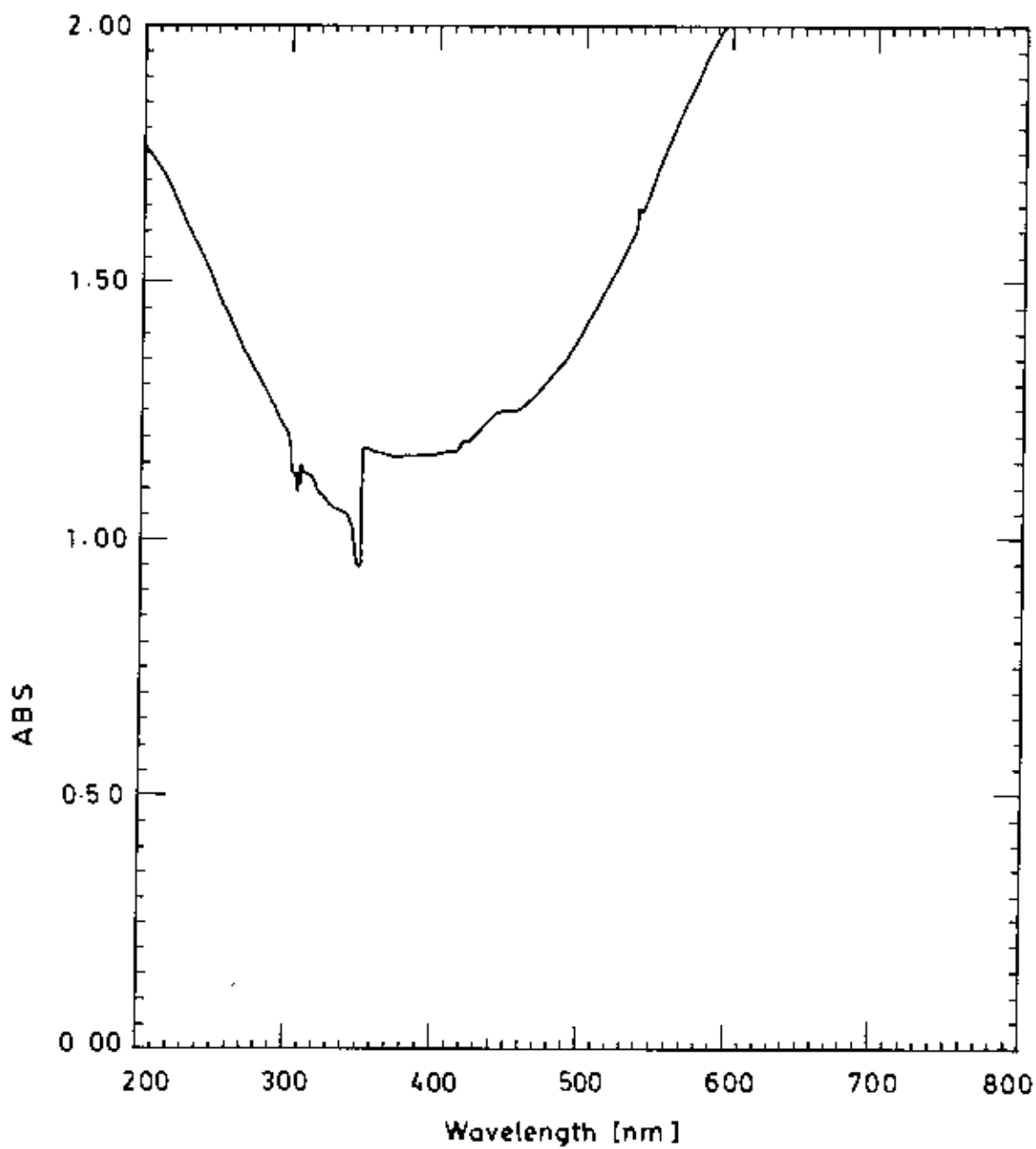


Fig. 4.1.d: UV - VIS spectroscopy for sample PP:Talc = 7:3

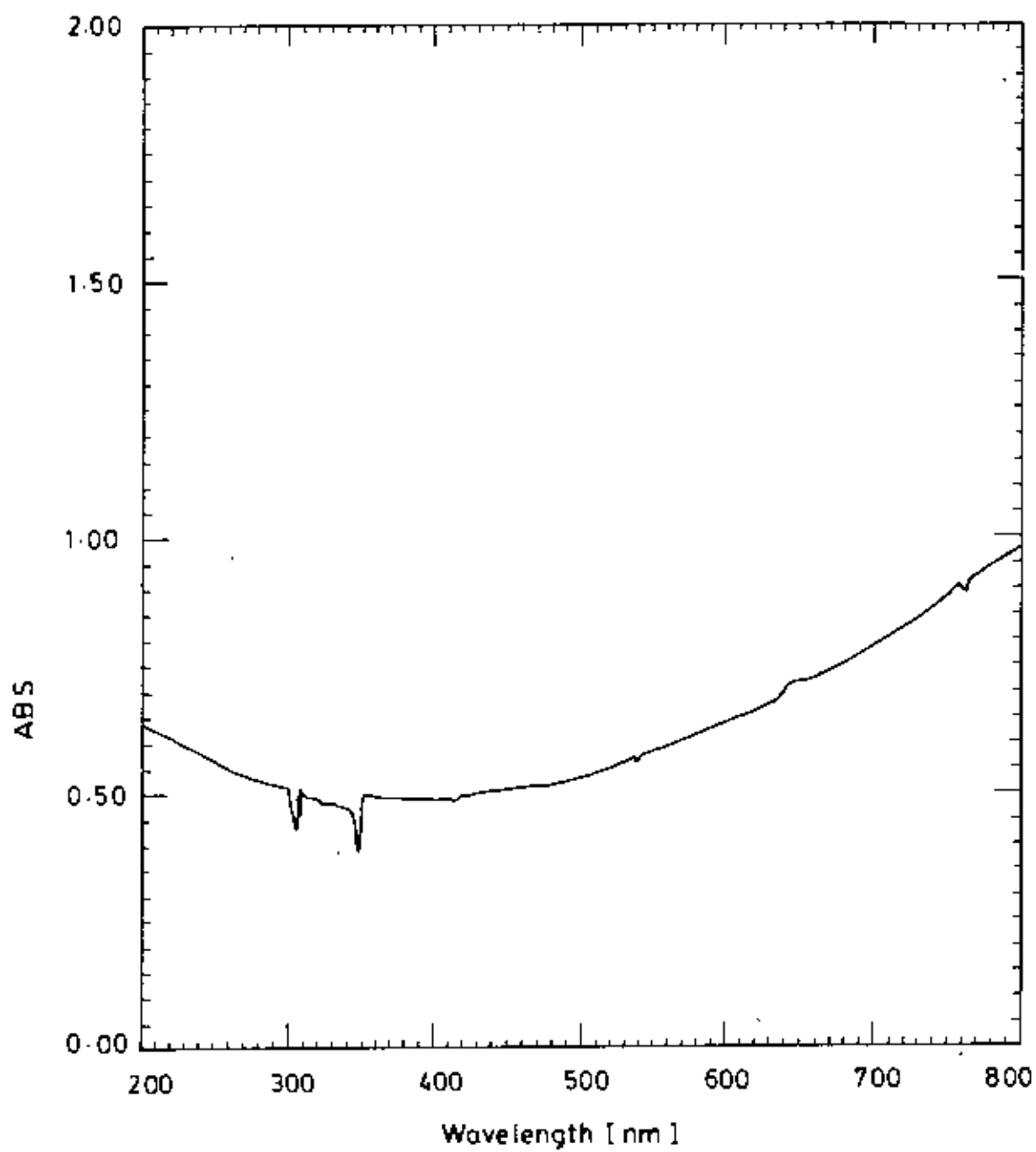


Fig.4.1.e: UV - VIS spectroscopy for sample PP:Talc = 6:4

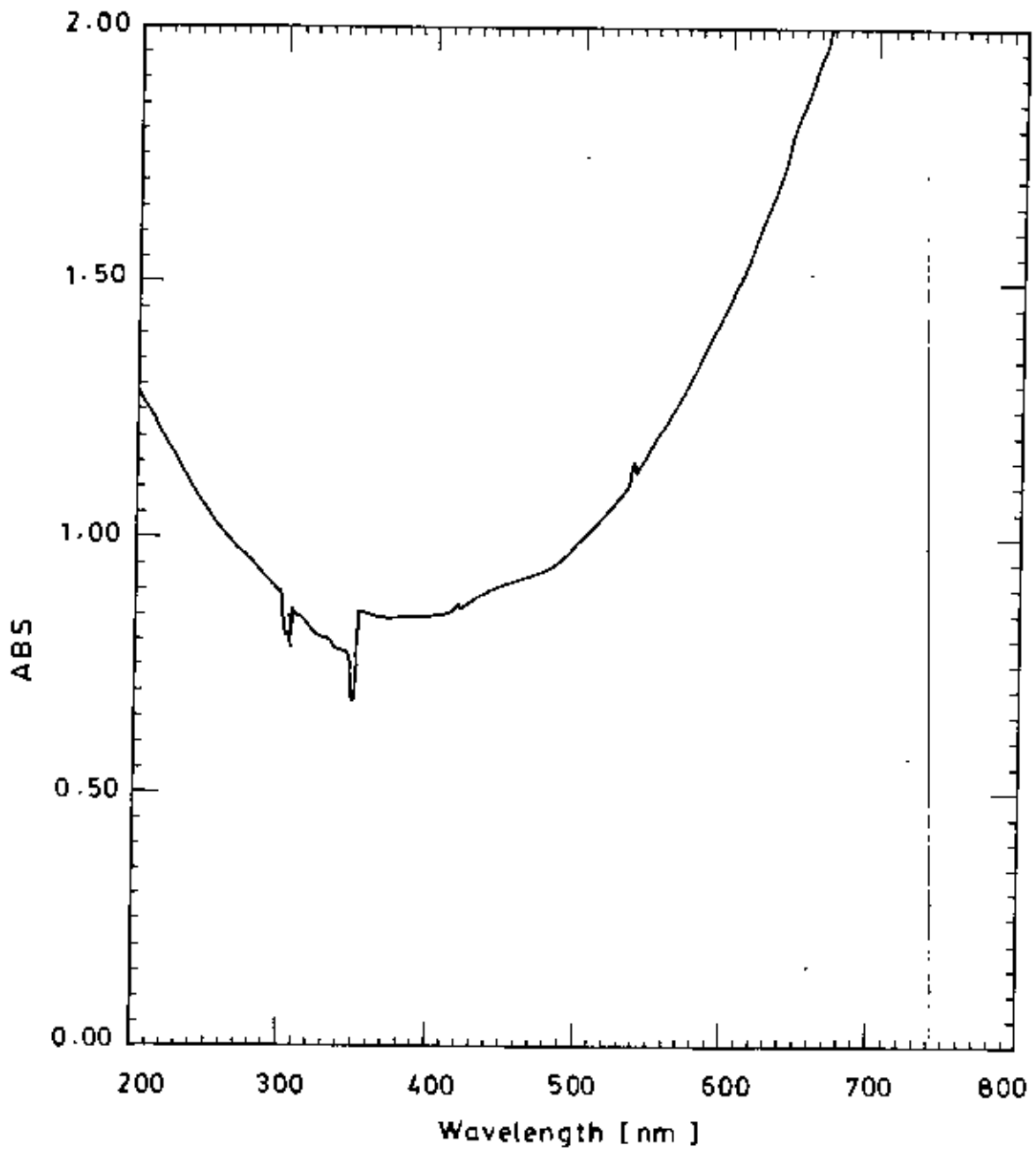


Fig.4.1.f: UV – VIS spectroscopy for sample PP:Taic = 5:5

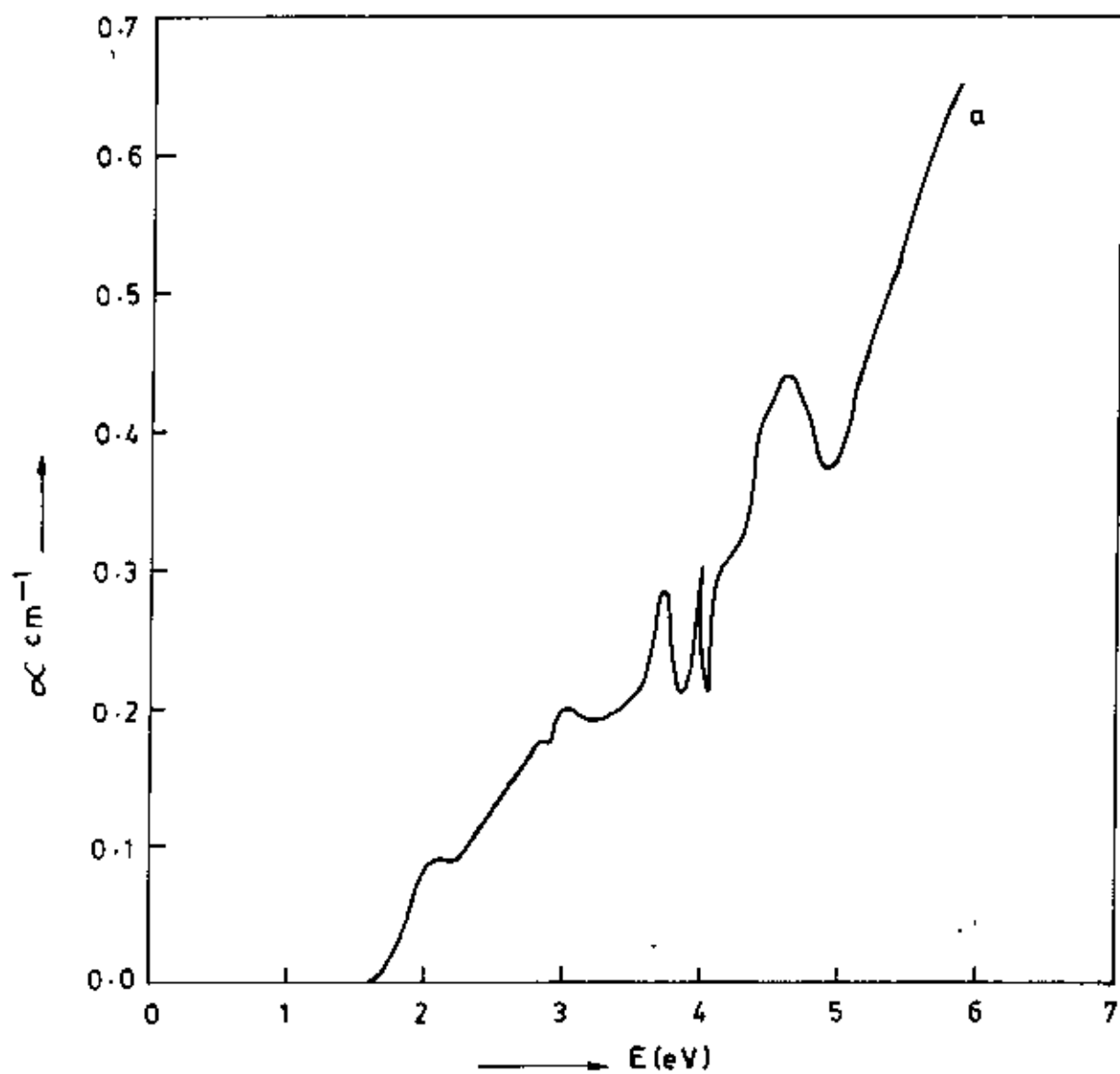


Fig.4.2: Plot of Absorption co-efficient versus photonenergy for sample pure PP

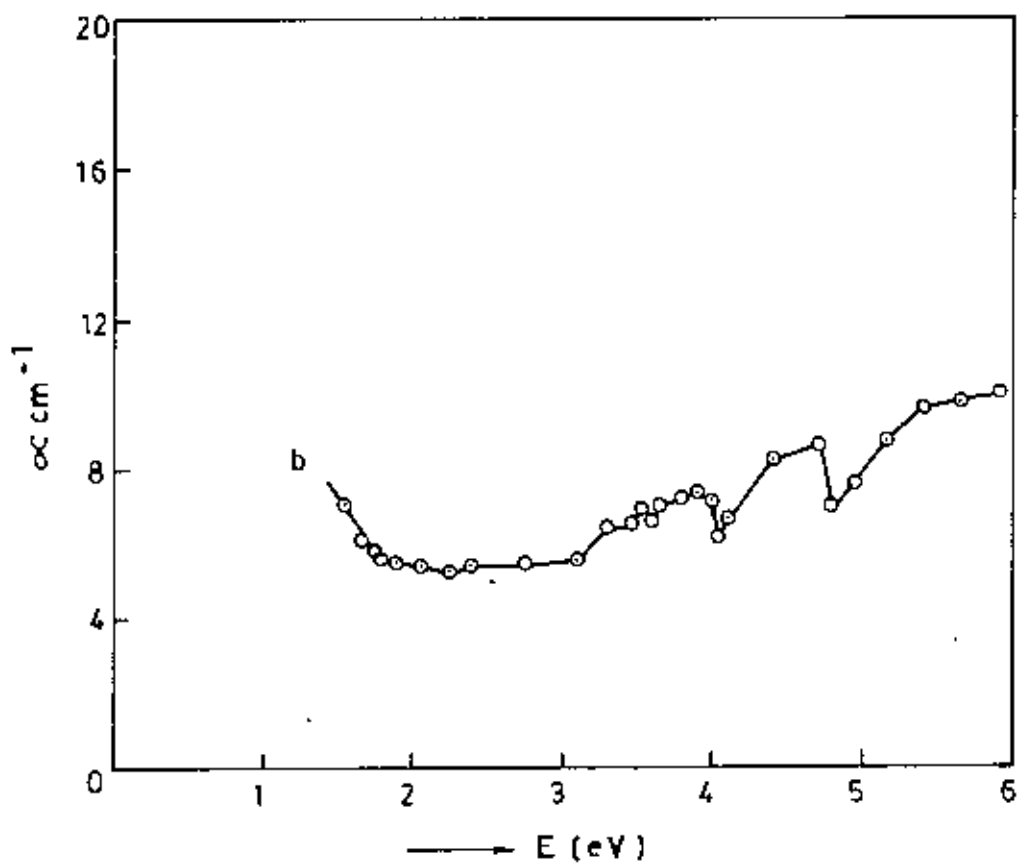


Fig. 4.2: Plot of Absorption co-efficient versus photon energy for sample PP : Talc = 9 : 1

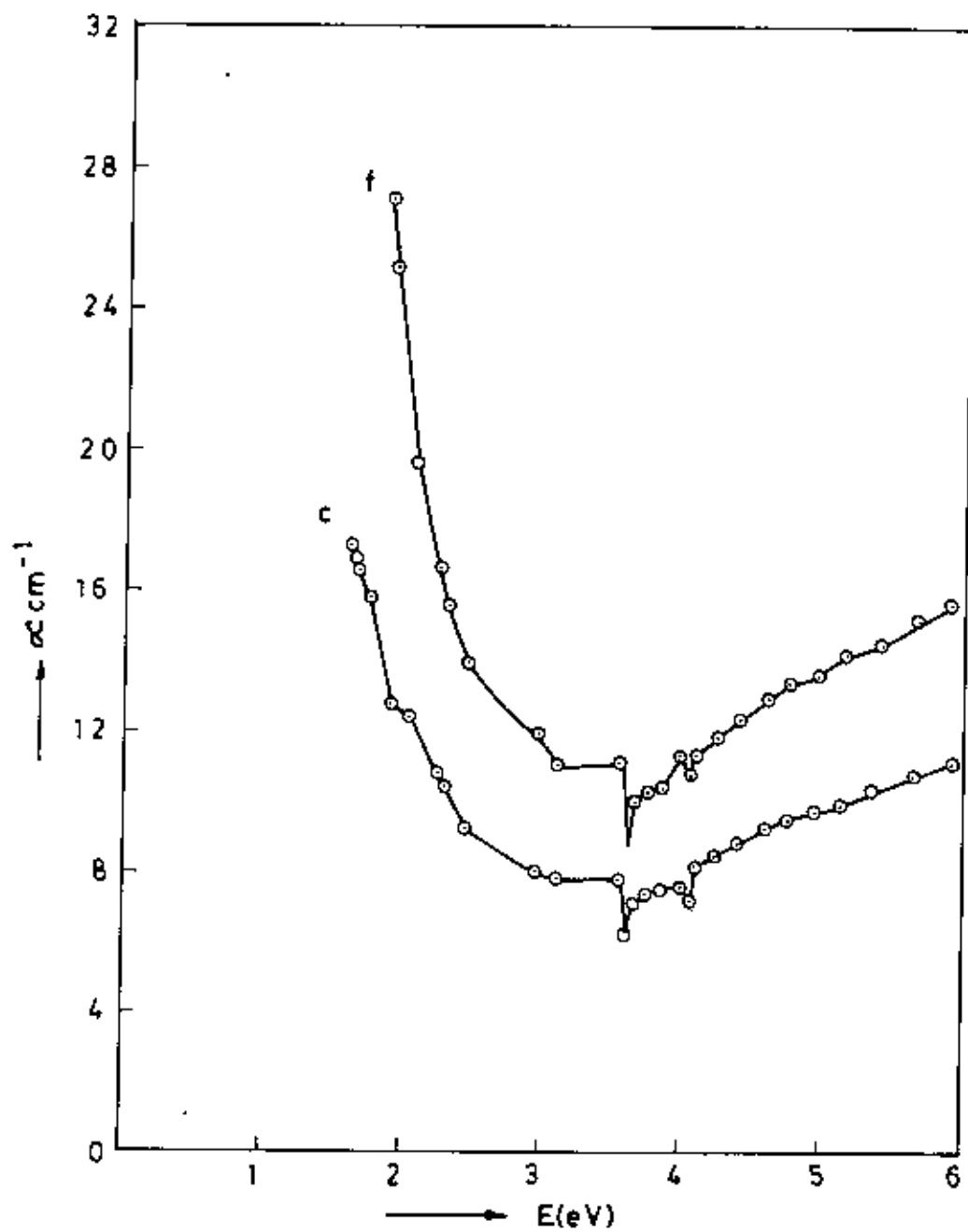


Fig. 4.2 : Plot of Absorption co-efficient versus photon energy for sample PP: talc = c) 8:2 and f) 5:5

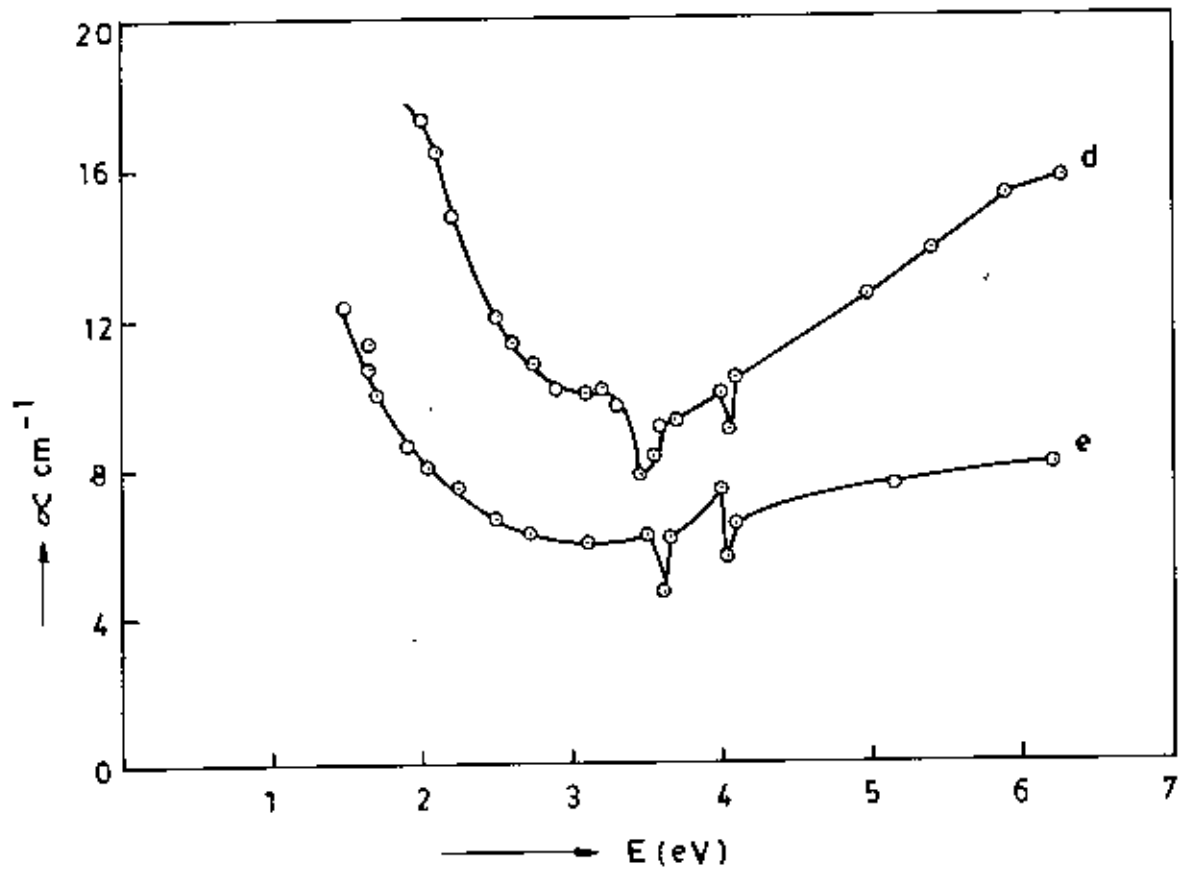


Fig.4.2: - Plot of Absorption coefficient versus photon energy for sample PP : Talc = d) 7:3 and e) 6:4 .

Table- I Bandgaps for different samples

Sample	E_g (eV)
Pure PP	1.60
PP:Talc = 9:1	0.90
PP:Talc = 8:2	1.00
PP:Talc = 7:3	0.75
PP:Talc = 6:4	0.90
PP:Talc = 5:5	0.80

4.2 Thermally Stimulated Depolarization Current (TSDC) measurements

4.2.1 TSDC spectra for pure PP

Fig. 4.3 shows the TSDC thermograms for different V_p and T_p of pure PP charged by high electric field injection. These are asymmetric in shape. Two discharge current peaks were observed with high intensity at the lower temperature region and low intensity at the higher temperature region in all the runs. However for both peaks, there may exist a distribution of relaxation times and activation energies.

Curve (a) in Fig. 4.3.x and curve (d) in Fig 4.3.y for $V_p=500V$ and $T_p=393K$ shows two broad peaks at about 323 and 410 K in the investigated temperature range. The maxima for PP could be connected with the release of free charge carriers from their traps depending on the polymer morphology [4.2]. The higher temperature peak may be attributed to deep charge trapping in the crystalline region and /or at the crystalline amorphous interfaces. The broad peak at 323K may be due to impurity and /or defect traps in the amorphous region distributed in energy. The possible existence of impurity and / or defects in PP was also observed in the UV-VIS measurements. P. Myslinski et.al.

[4.3] reported TSDC and dielectric properties of PP-Polycarbonate blends . In their investigation, they observed two maxima at about 338K and 293K in the TSDC thermogram of PP. Charge trapping and conduction in pure and iodine-doped biaxially oriented PP (BOPP) were studied by P. Karanja and R. Nath [4.1]. They found that the two maxima occurred at about 361 and 393K in BOPP. K. Shindo [4.4] investigated the charge migration in PP and polyethylene terephthalate (PET) by TSDC and TSPC measurements . They observed a single peak at about 430K in PP . The deviation of the reported results from the results of the present investigation is obvious . Because the above mentioned reports were based on different measurement conditions and different types of PP. Even then the results obtained in the present study have some correlation with the reported ones as far as charge trapping in the lower and higher temperatures are concerned.

It is seen in the TSDC thermograms for constant V_p at various T_p 's and for constant T_p with various V_p 's that the high temperature peak is more affected compared with the low temperature peak. The dependence of the high temperature peak and the low temperature peak maxima on V_p and T_p may be due to the interfacial and dipolar polarization respectively. This fact will be discussed again in the following sections.

4.2.2 TSDC spectra for composites

The TSDC thermograms of the five composites of PP- Talc at different V_p and T_p are presented in Figs. 4.4 - 4.8. It is seen that in all the spectra, the general feature is the same as that of pure PP. It is seen that the low temperature peak maxima shift to the region 285 - 310K and the high temperature peak maxima shift to 400K and below. The low temperature peak of the composites are away towards low temperature side from the low temperature peak of PP. Thus it may be assumed that these peaks are due to the charge motion for the addition of Talc in PP.

It is observed that with the increase of the amount of Talc in PP, the low temperature peak maxima has appeared between 285 and 310K weekly sensitive to V_p and T_p whereas

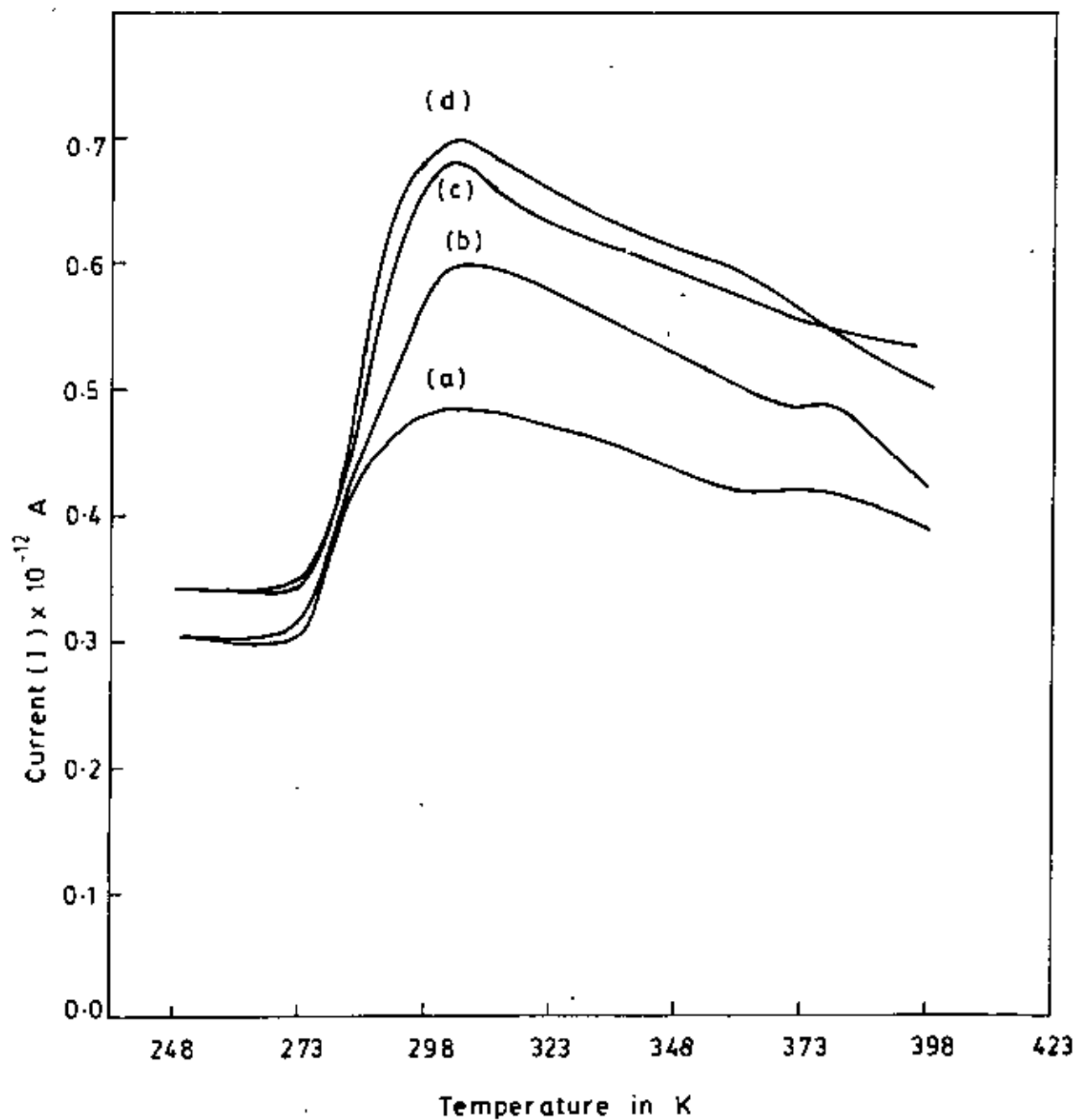


Fig. 4.4.y: Typical TSDC curves for sample PP:Talc = 9:1

$V_p = 500V$

$T_p =$ a) 333K

$t_p = 15 \text{ min}$

b) 353K

c) 373K

d) 393K

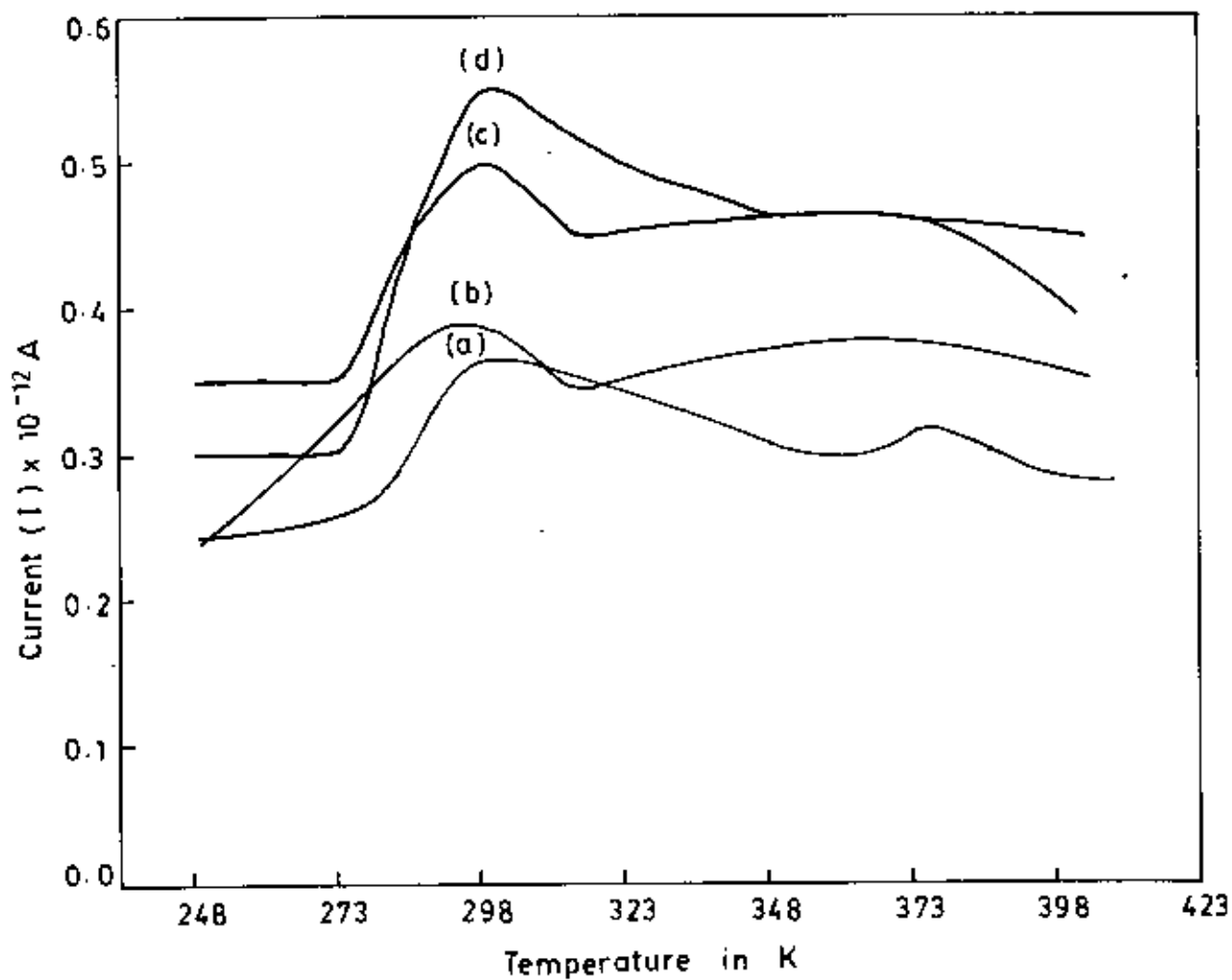


Fig.4-6.y: Typical TSDC curves for sample, PP:Talc = 7:3

$V_p = 500V$, $T_p =$ a) 333 K $t_p = 15$ min
 b) 353 K
 c) 373 K
 d) 393 K

the high temperature peak becomes weaker. This weakening of the high temperature peak could be understood by inferring that Talc may take place at the crystalline - amorphous interfaces and in the crystalline region which presents space charge trapping at these sites and thus lead to the weak intensity band at about 400K. It is also seen that this peak appears again on annealing in all the composites. This suggests that those charges injected from the electrodes are somehow captured by Talc and no longer able to accumulate in the semicrystalline region of PP i.e. the composite may change towards the semicrystalline morphology as that of the pure PP.

To see at a glance, TSDC spectra of the composites together with that of PP at $V_p = 500V$ and $T_p = 393K$ for $t_p = 15$ min are shown in Fig. 4.9. It is observed that both the peaks shift to the low temperature with the increase of Talc content (wt%) in PP. The low temperature peak does not change much whereas the high temperature peak becomes broad and weak. For further understanding, the dependence of the total released charge Q , with Talc contents and V_p will be discussed in the next section.

4.2.3 Dependence of the total charge Q released on the V_p and Talc content (wt%)

Integrating eqn. (2.5) (chapter II) over a wide range of temperature yields the total charge released from the electrodes during the course of the movement of charges. Thus the total charge, Q , liberated during a TSDC run can be obtained using the following expression.

$$Q = \int_{t_1}^{t_2} J_D(t) dt \quad (4.1)$$

where $J_D(t)$ is current density of the charge released from a sample during the heating over a time period t_1 to t_2 . For the case of dipole orientation eqn (2.2) (chapter- II) shows that the charge will be linear in the polarizing voltage. TSDC may also result from the motion of space charge injected into the insulation during polarization. In general, one

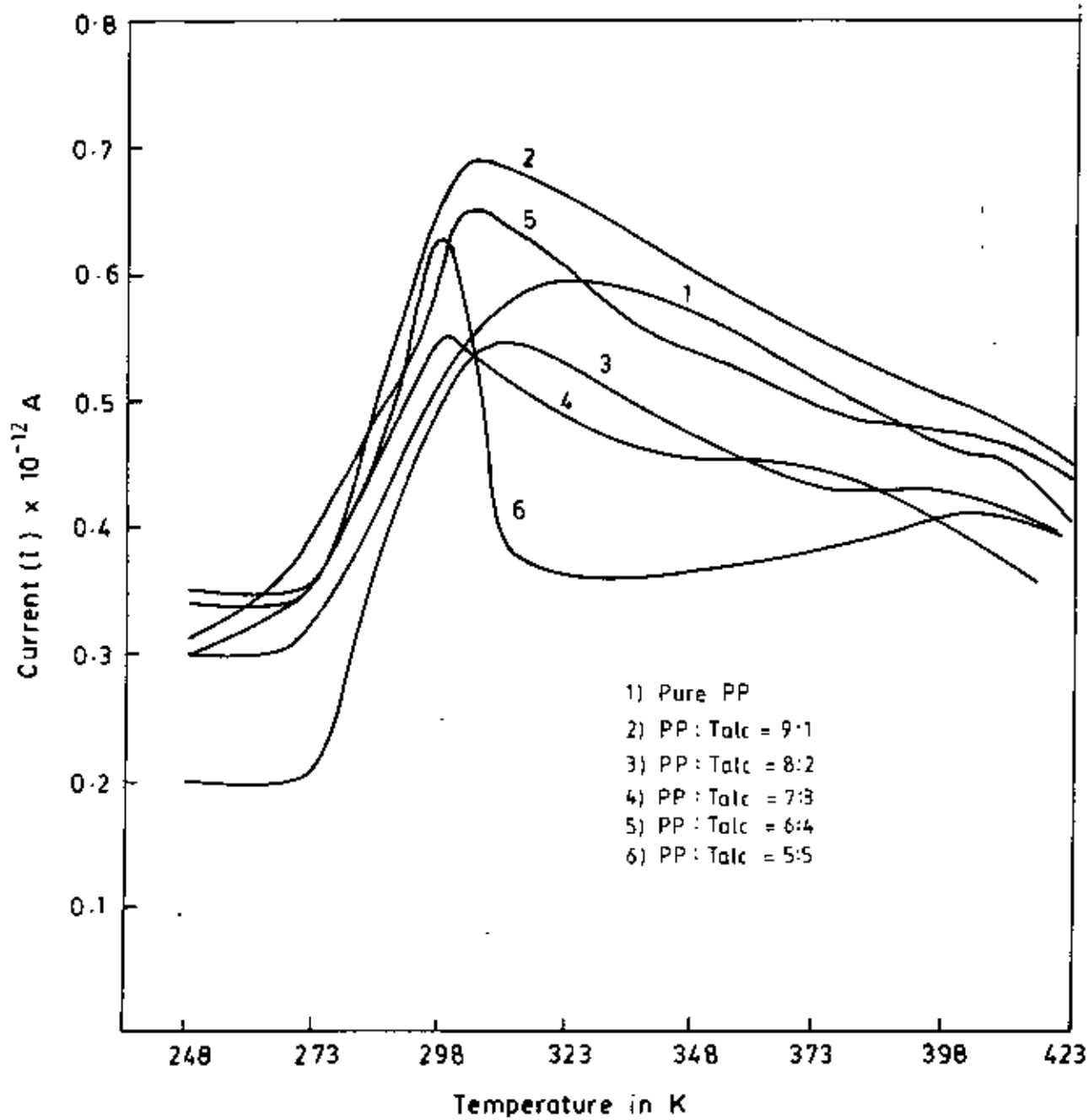


Fig. 4.9: Typical TSDC curves for different samples at $V_p = 500\text{ V}$ and $T_p = 393\text{ K}$

does not expect a linear relationship between charge released and polarizing voltage for TSDC due to space charge motion [4.5]. The dipoles may be true molecular dipoles or they may be the result of interfacial polarization (Maxwell - Wagner effects) or charge hopping in a double well potential.

The areas under the low temperature peak (285 - 323K) of the TSDC curves of all the samples were measured following eqn. 4.1 in order to obtain the total released charge, Q . A plot of Q versus the polarizing voltage V_p is presented in Fig. 4.10. This plot shows that Q can reasonably be related to V_p linearly which suggests that the peak is due to dipole relaxation. Thus a possible mechanism is the displacement of ions within the silica sheets of Talc. In order to see the effect of Talc content (wt%) on the charge storage in PP, Q versus Talc content (wt%) in PP was plotted and are presented in Fig. 4.11. It is seen in Figs. 4.10 and 4.11 that Q increases linearly with V_p in all the investigated composites whereas Q tends to decrease with Talc (wt%) in PP at all the polarizing voltages. The tendency of decrease of the Q with Talc content (wt%) may be due to increased repulsion force between the cations at the higher Talc concentrations.

The peak current I_m was plotted against V_p and Talc content (wt%) in PP and is shown in Fig 4.12.x and 4.12.y respectively. It is seen in these figures that, the I_m increases with polarizing voltages, V_p , whereas I_m seems to be poorly dependent on Talc content (wt%) with a minimum at about 30 wt % Talc.

4.2.4 Activation energy from TSDC

The activation energy of the trap levels may be determined in different methods [4.6] as described in Chapter- II. The initial rise method gives a good estimate of activation energy of TSDC when no obscuring effects from shallow traps are present on the initial rise. For this reason, the initial rise technique may not provide an accurate estimate of the activation energy of a TSDC containing multiple peaks. In such cases, the activation energy is calculated using the theories based on the temperature intervals in which $J_D(T)$

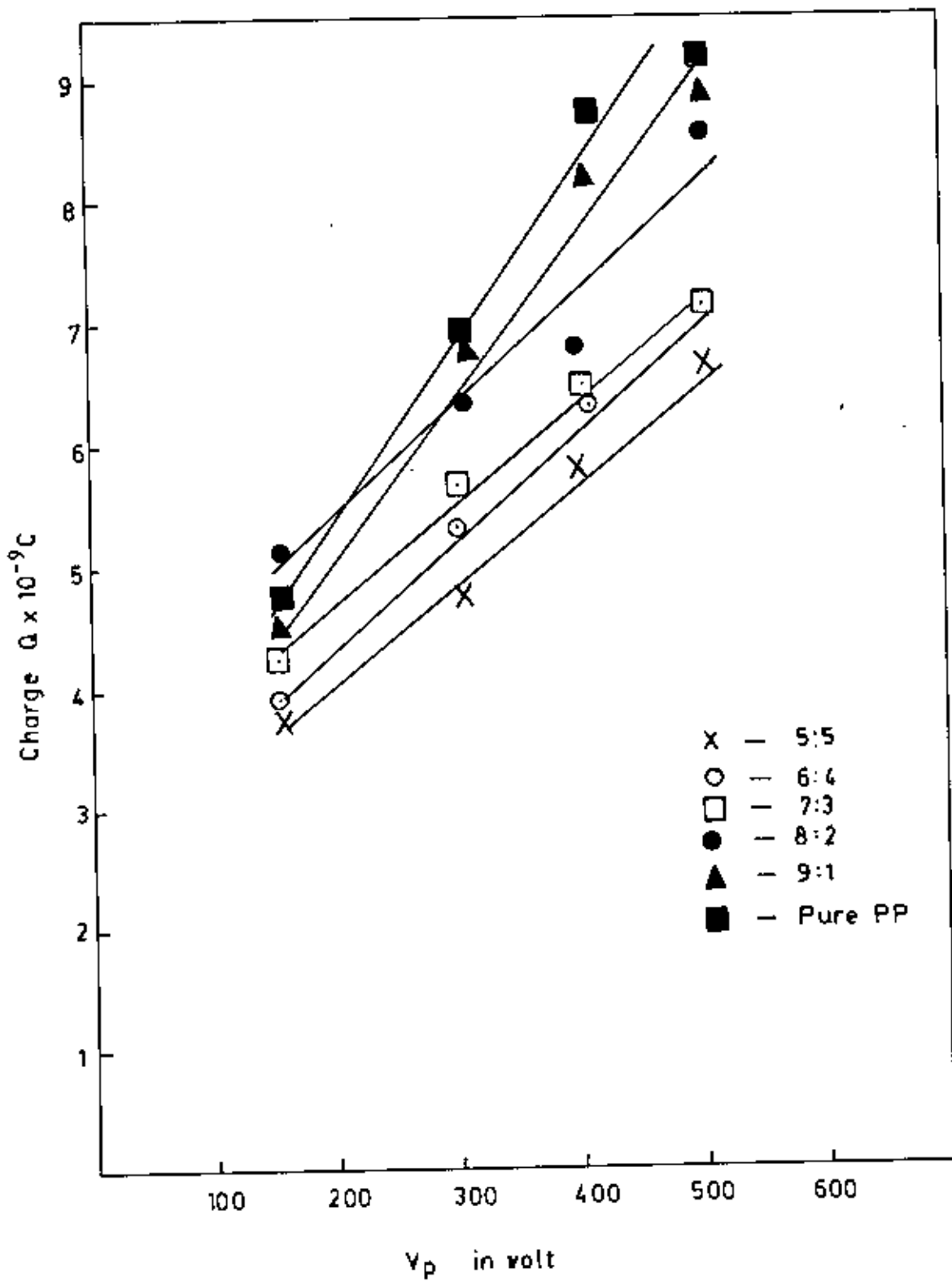


Fig. 4-10: Plot of Q versus V_p for different samples

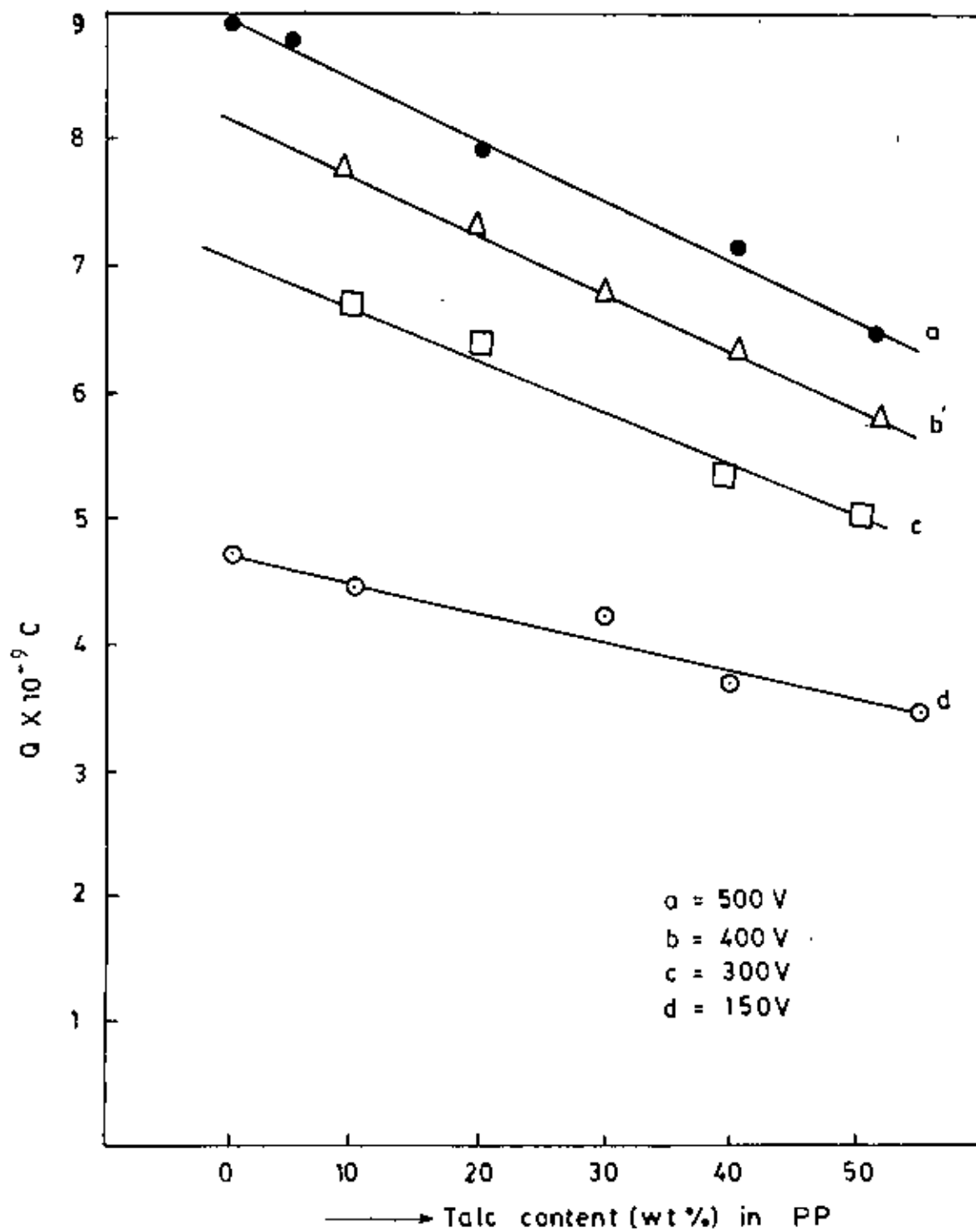


Fig. 11 Plot of Q versus Talc content (wt %) in PP

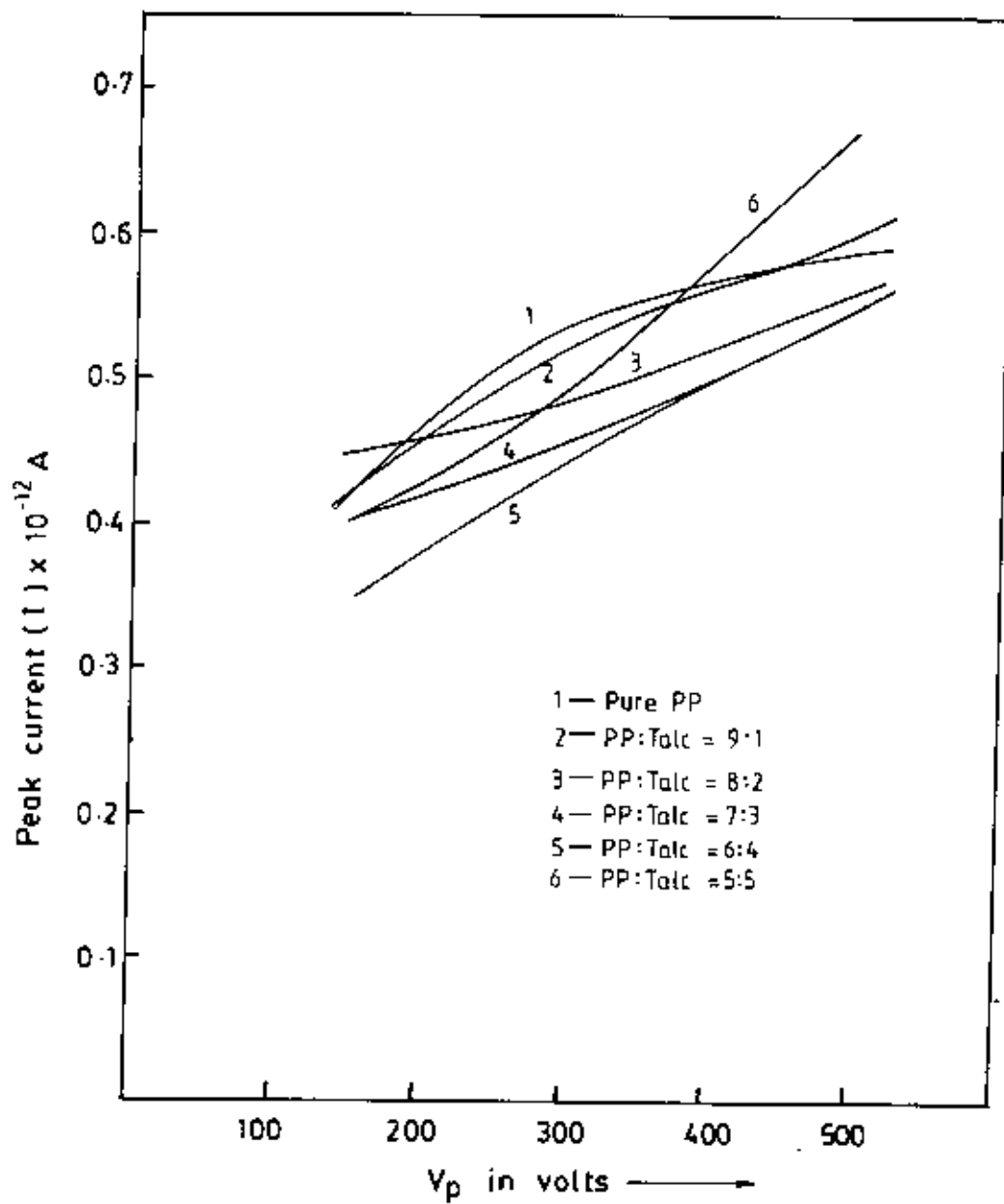


Fig. 4.12.X. Plot of peak current versus V_p for all samples

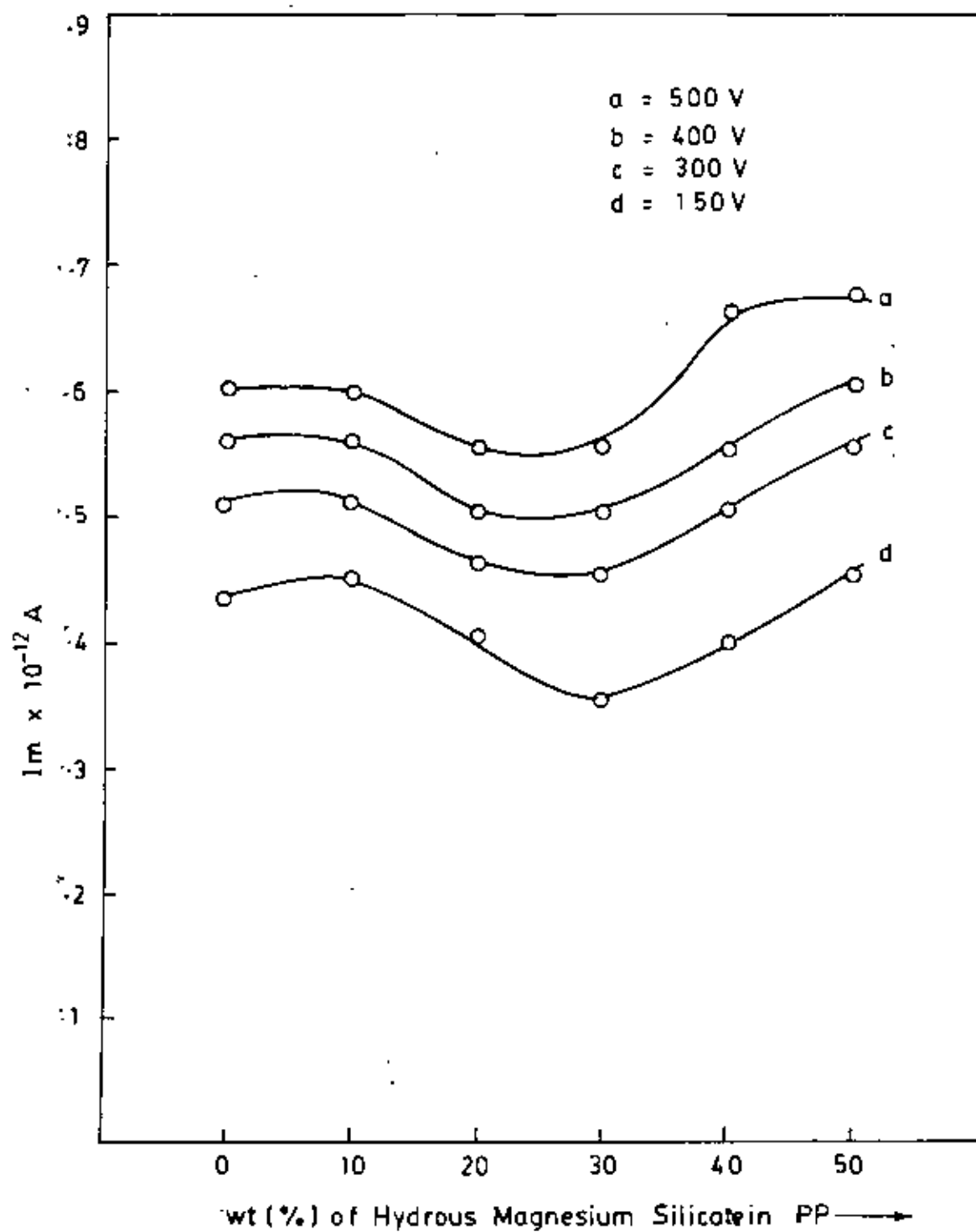


Fig. 4.12.y: Plot of maximum peak current versus wt (%) of Hydrous Magnesium Silicate in PP at fixed $T_p = 293 K$ for different voltages.

passed between the half maximum and full maximum value. Thus, the activation energy is given by Grossweiner [4.7]

$$E = 1.51 \frac{kT_1 T_m}{T_m - T_1} \quad (4.2)$$

where T_m is the peak temperature and T_1 is the temperature at which the peak half height occurs in the increasing part of the curve. The activation energy values obtained for the low temperature peak by using formula (4.2) for all samples are documented in the appendix.

The activation energy for pure PP is about 0.45 to 0.60 eV and that for the composites is about 0.50 to 0.87 eV. The activation energy increases with the increase of Talc (wt%) in PP. The studies on Zeolite filled low density polyethylene (LDPE) by TSDC reported the values of the activation energies 0.45 to 0.50 eV[4.8]. In this paper the authors argue that the dipolar polarization is due to the dipole formed between the positive ions in the zeolite cage and the form of the zeolite itself which is negatively charged. In the PP-Talc composites, the dipole may be formed between the Mg^{++} ions situated between the two silica sheets and the O^- ions situated on the surface of the Talc sheets-Fig. 1.3. This dipole polarization is affected by the surrounding polymer.

References of chapter - IV

- 4.1 P. Karanja and R.Nath, IEEE Trans. Dielectr. and Electr. Insul., 1 (1994)213-223.
- 4.2 P. Myslinski and M. Kryzewski, Polym. Bull.2 (1980) 761.
- 4.3 P. Myslinski, Z. Dobkowski and B. Krajewski "Electrical properties of polypropylene-polycarbonate Blends" in the book Polymer blends processing, morphology and properties Vol. 2, edited by Marian Kryszewski, Andrzej Gateski and Ezio Martuscelli. Plenum Press ,NY, (1984)157-163.
- 4.4 Kimio Shindo, IEEE Trans. Dielectr. and Electr. Insul., 24 (3) (1989) 481-488.
- 4.5 J. van Turnhout, "Thermally stimulated discharge of Electrets" in Topic in Applied Physics: Electrets, Vol 33, G.M.Sessler ed., Springer-Verlage, NY, 1980.
- 4.6 J. Vanderschueren and J. Gasiot, "Field induced thermally stimulated currents" in Topics in Appl. Phys. Vol. 37, P. Braunlinch (ed.) Thermally stimulated relaxation in solids Springer-Verlag, 1979, N Y. p- 135 - 223.
- 4.7 I. I. Grossweiner, J Appl. Phys. 24 (1953) 1306-1307.
- 4.8 W. Yin, J. Tanaka and D. H. Damon, IEEE trans. Dielectr. and Electr. Insul., 1 (1994) 169 - 180.

CHAPTER-V

CONCLUSIONS

5.1 Conclusions

5.2 Suggestions for further study

Appendix

Chapter-V

Conclusions

5.1 Conclusions

In this work the PP- Talc composites with different composition of PP and Talc were prepared by extrusion technique . Since the electrical , optical and other properties of a two-phase composite material depend on both the type and weight/ volume fraction of the filler and the matrix and their interaction, this project was undertaken to study the PP-Talc composites as an electret. For this purpose, the UV-VIS absorption and TSDC measurements were performed on PP and five different PP-Talc composites. From the obtained results, the following conclusions can be drawn.

The absorption increases with Talc content (wt%) in PP whereas the bandgap decreases. The absorption spectra show the presence of impurity and / or defect traps in the matrix.

At the low temperature, charge releases from the impurity and / or defect traps in the amorphous regions of the polymer PP and at high temperature, charge releases from the deep charge trapping sites in the crystalline-amorphous interface.

Analysis of the TSDC curves of the composites yields that the low temperature peak in the composite is due to the dipolar relaxation in the Talc. There may be some contribution from the trapping sites of the polymer PP. The total charge released, Q , has a decreasing tendency with the Talc content (wt%) which may be due to the repulsion force between the cations. Reduction of intensity of the high temperature peak may be due to the existence of Talc in the crystalline-amorphous interface which compensates the charges to be released. The maximum activation energy for the PP is 0.60 eV and for the composites is 0.85 eV.

5.2 Suggestions for further study

In this thesis an attempt was made to investigate one of the electrical properties, the charge storage and charge relaxation in Talc based PP-composites. In future, the structural, dielectric and mechanical properties of these materials should be studied. Again, the above investigations with different fillers and different filler size will be of much help to understand the effect of filler type and structure and their interaction with matrix polymer PP.

Appendix

Values of Q , I_m , T_m and E

Sample	Polarizing voltage V_D Volt.	Charge $Q \times 10^{-9}$ Coul.	Peak Current $I_m \times 10^{-12}$ A	Peak Temp. (T_m) in K	Activation energy E (eV)
Pure PP	500	9.00	0.59	323	0.442
	400	8.90	0.56	315	0.467
	300	6.90	0.54	303	0.428
	150	4.70	0.44	308	0.599
PP : Talc = 9:1	500	8.90	0.60	303	0.520
	400	7.07	0.56	303	0.635
	300	6.70	0.52	303	0.652
	150	4.47	0.44	304	0.666
PP : Talc = 8:2	500	8.66	0.55	310	0.621
	400	6.74	0.50	303	0.638
	300	6.32	0.46	298	0.572
	150	5.29	0.40	285	0.832
PP : Talc = 7:3	500	7.07	0.55	298	0.721
	400	6.44	0.50	308	0.796
	300	5.66	0.45	298	0.732
	150	4.18	0.35	298	0.791
PP : Talc = 6:4	500	7.07	0.55	303	0.821
	400	6.32	0.45	298	0.812
	300	5.29	0.44	310	0.865
	150	3.87	0.40	285	0.872
PP : Talc = 5:5	500	6.63	0.67	285	0.880
	400	6.00	0.60	298	0.832
	300	4.74	0.45	330	0.872
	150	3.87	0.45	283	0.868

